https://ntrs.nasa.gov/search.jsp?R=19700002880 2020-03-12T04:45:48+00:00Z

N 70 12184
NASA CR 107027

# FINAL REPORT

# A CORRELATION OF OPTICAL, RADIO, AND INTERPLANETARY RECORDS OF SOLAR EVENTS

LMSC 687340

June 1968

CASE FILE COPY

Lockheed

PALO ALTO RESEARCH LABORATORY

LOCKHEED MISSILES & SPACE COMPANY • A GROUP DIVISION OF LOCKHEED AIRCRAFT CORPORATION

PALO ALTO, CALIFORNIA

FINAL REPORT

# A CORRELATION OF OPTICAL, RADIO, AND INTERPLANETARY RECORDS OF SOLAR EVENTS

LMSC 687340 June 1968

Sara F. Smith
and
Karen L. Angle

Lockheed Solar Observatory

Photographic Illustrations
by

B. Nolan

Submitted to the National Aeronautics and Space Administration
upon completion of Contract NASw 1690

LOCKHEED MISSILES & SPACE COMPANY

CONTENTS

FIGURES

# Section 1
# INTRODUCTION

The aim in this investigation of solar events has been to study the details of optical flares and to ascertain which aspects might be reflected in x-ray radio, or interplanetary particle events. It is well known, of course, that most major flares can be also observed as x-ray, radio, and particle events. In the light of Hydrogen-alpha alone, however, a major flare is a composite of many phenomena. Flares may be composed of numerous bright points, hazy emission and ejected material. They may be associated with filament eruptions, shock waves, loops, and surges. Furthermore they may display several characteristic stages of development from an initial ascendance of a filament, to the start of emission, the flash phase and often multiple maxima in brightness. Finally they end with a gradual decay of the bright emission remaining in the chromosphere. It is felt that an accurate model of the flare process cannot easily be constructed until more is learned about which of these aspects are related to the various non-optical observations of flares.

In this report, we first describe the observations of some significant details of flares which have received insufficient attention and which are critical to the understanding of solar flares. Then we describe our attempts to relate these details to specific characteristics of x-rays, radio bursts and, to a lesser extent, particle events. Hopefully this study will contribute to a better general understanding of solar flare processes.

# Section 2
# SIGNIFICANT CHARACTERISTICS OF THE OPTICAL FLARE IN H-ALPHA

## 2.1 Flare Points

On filtergrams or spectroheliograms exposed for disk structure in the center of the H-alpha line, it is difficult to resolve fine structure in flares. Observers frequently note that several flare pieces may begin within a few seconds or minutes of each other at separate locations within an active region. In most flares several of the separate initial flare pieces merge together into one or more larger segments during the rapid rise of a flare to maximum intensity (Hyder 1967, Dodson and Hedeman 1968). Occasionally, faint or small flares occur in which additional structure can be observed at normal exposures for the chromosphere. Such a flare is illustrated in Figures 1 and 2. In Figure 2, long exposures were used in making the prints to further emphasize the flare structure.

The flare in Figure 2 appears to be composed of elongated bright points connected by fainter strands of emission. As the flare builds, additional bright points and connecting strands form while the initial points decay. The significant aspect of this process is that the individual flare points have very short lifetimes. In this event many of the small flare points have a duration of less than 3 minutes. The formation of new points continues until nearly the end of the flare. After the flare has attained maximum intensity and area, around 1814 U.T., the rate of formation of new flare points gradually decreases. The larger and apparently longer-lived segments appears to result from a coalescing of smaller flare points. It is further noted that these larger flare pieces do not symmetrically increase in area but instead show small nodules along some of the advancing borders. Also, the initial flare points in these coalesced segments tend to be the first locations where the intensity drops off.

# 1 AUG 66

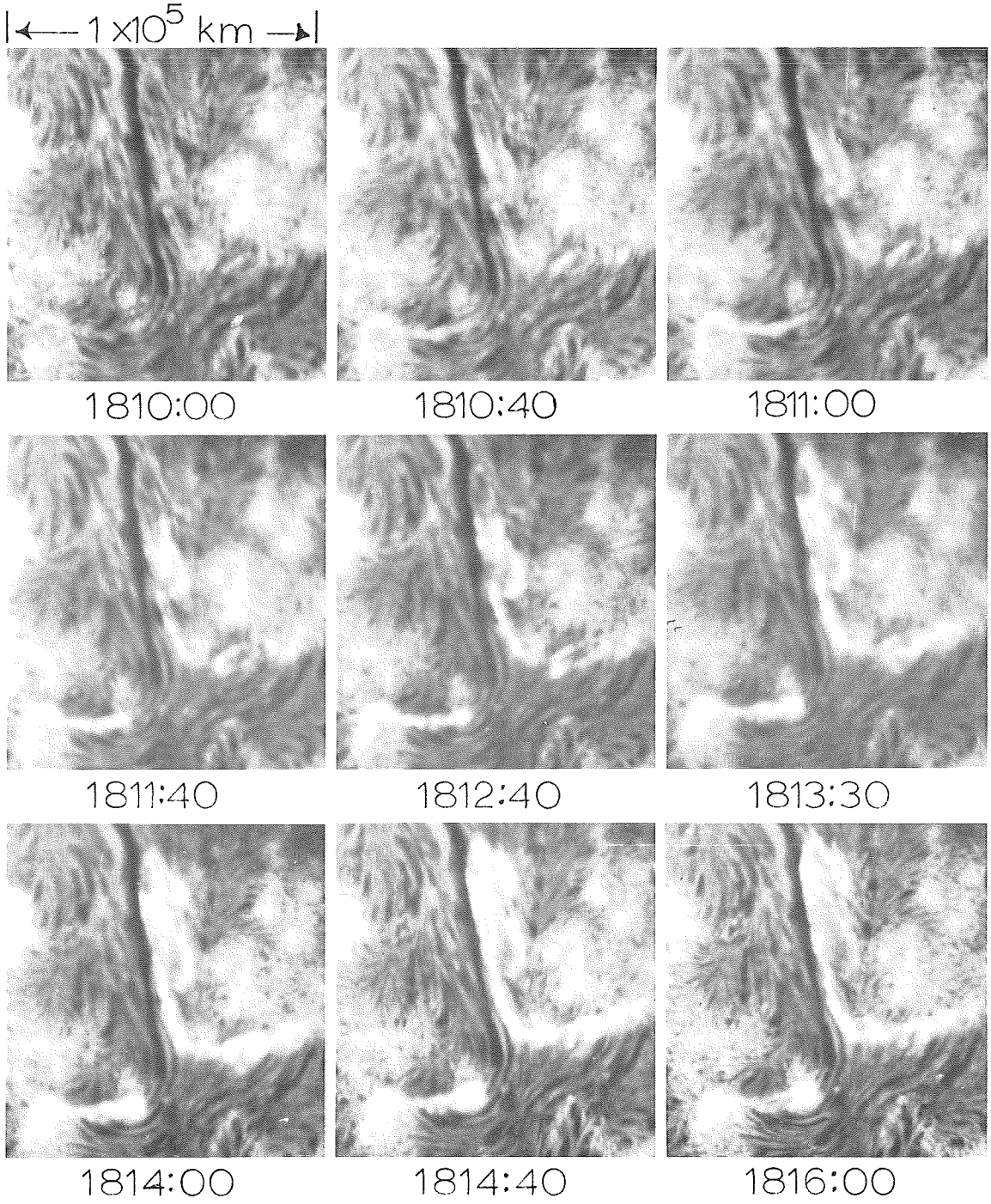


Figure 1. As this flare develops, structures surrounding the flare points show no visible change even as close as 1 or 2 seconds of arc to the flare emission. Even the filament adjacent to the flare remains unchanged from flare effects.

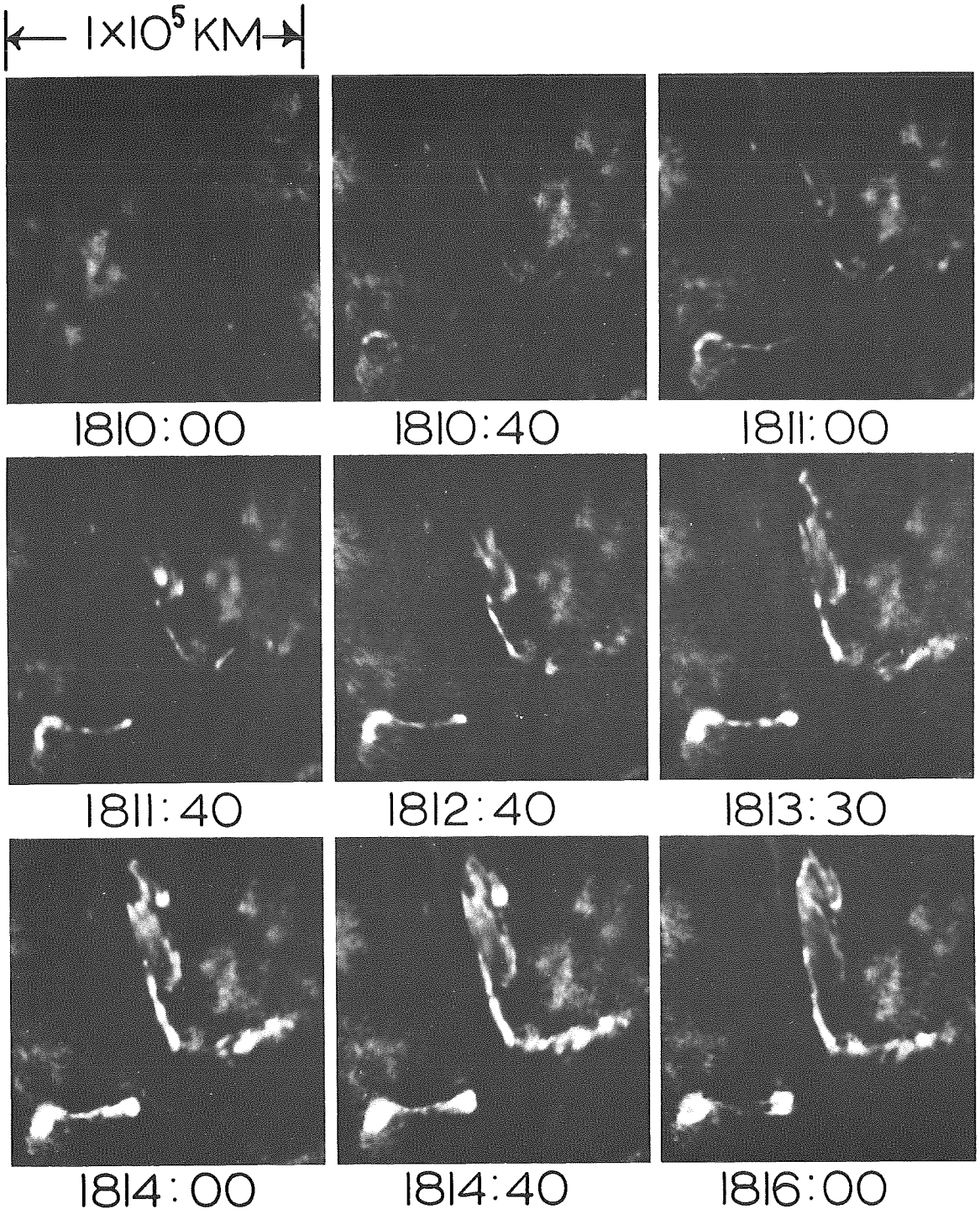


Figure 2. In these overexposed prints, the flare is composed of bright points connected by fainter strands of emission. Lifetimes of the smaller flare points are frequently less than 3 minutes.

In normal exposures for the chromosphere (Figure 1) there is no evidence that these flare points in any way disturb adjacent areas of the chromosphere even as close as 1 or 2 seconds of arc distant. In Figure 2, the smallest resolved flare points are on the order of a sec of arc in diameter. Most of the flare points occur where bright plage previously existed, and consequently where the longitudinal component of the local magnetic field is relatively strong (Ramsey and Smith 1969 unpublished).

Photographs of flares in the wings of H-alpha bring out another salient feature of flare points. They are consistently brighter in the red wing than in the blue wing of H-alpha at any given time (Ramsey, Smith, and Angle 1968). This characteristic is clear in small flares such as the one illustrated in Figure 3 taken at H $\alpha \pm 1.1$Å. It has not been established definitely whether this red wing asymmetry in flare points and flares (Ellison 1949) is due to Doppler shifts or to an asymmetric broadening of the line due to effects of collision. In the filtergrams it is clear that this asymmetry can not be explained by overlying absorption in the blue wing as was originally proposed.

Observations of flare points in real time from video tapes taken in the center and wings of H-alpha also have yielded information on the initiation and duration of flare points in small flares. At H $\alpha$ + 2.5Å flare points abruptly appear and reach saturation in intensity within 2 to 5 seconds (Ramsey, Smith, and Angle 1968). The lifetimes of flare points at H $\alpha$ + 2.5Å varies from several seconds to several minutes.

All of these aspects of flare development are in agreement with the idea that one of the primary processes in flares is one which results in a continuous formation and decay of tiny, short-lived, bright points rather than a progressive excitation of adjacent chromospheric material resulting from an initial instability at one or more points. The lack of disturbance of the chromosphere around flare points and the existence of

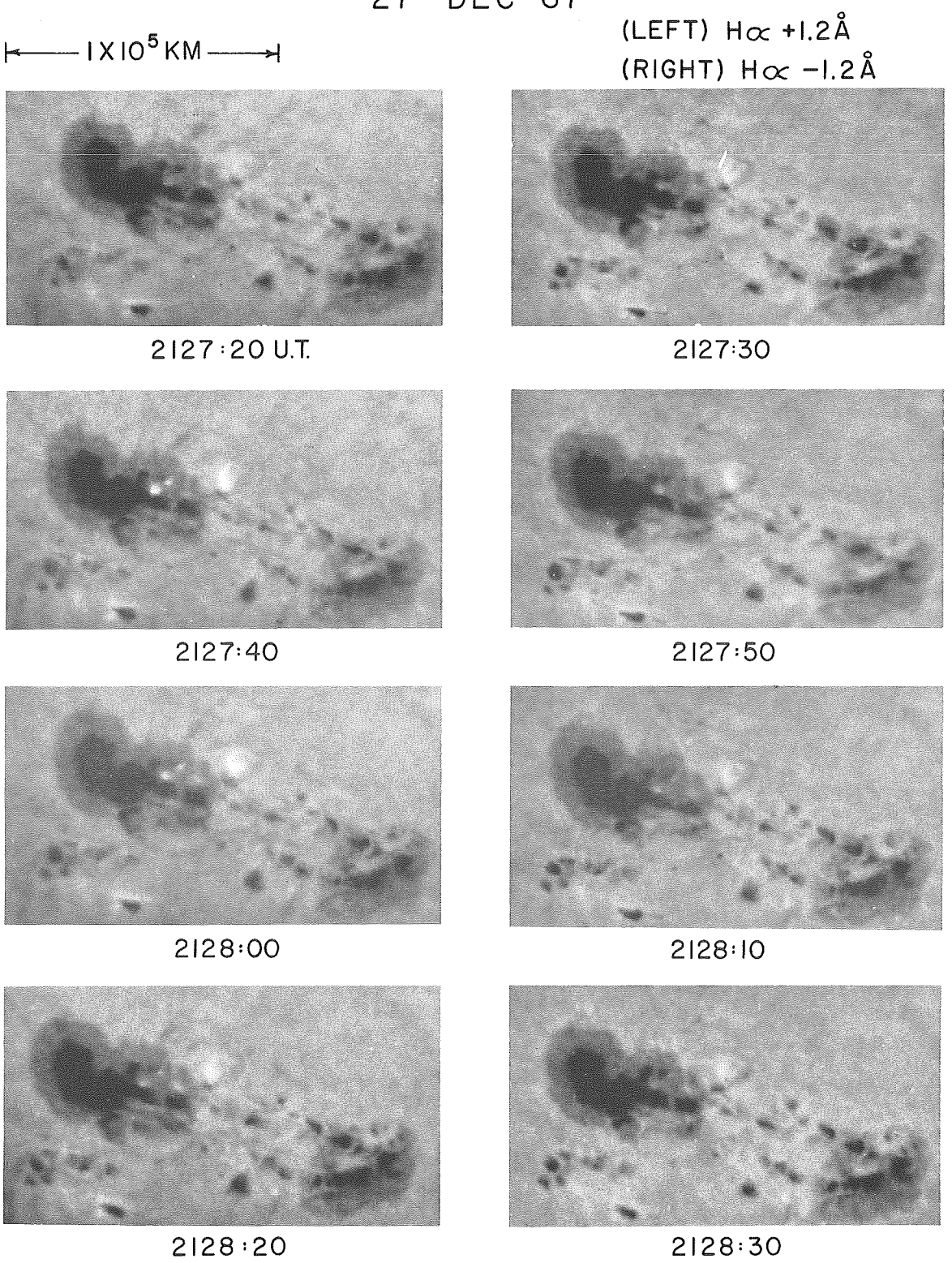


Figure 3. Flare points in the wings of Hα distinctly show an asymmetry favoring the red wing of the line. This red wing asymmetry is typical of flares in Hα (Ellison 1949).

a strong longitudinal component of the local magnetic field at flare locations suggests that the flare emission in the chromosphere is being triggered in the corona above the active region, perhaps by high energy particles streaming downward along field lines and colliding with the chromosphere to produce the observed emission in H-alpha.

## 2.2 The Explosive Phase Versus the Flash Phase in Flares

Early in the rise-phase of flares there is a stage of development which sometimes can be determined with an accuracy of 30 seconds. This stage is the start of explosive phase of the start of flash phase of a flare. The term "flash phase" was first used by Ellison (1949) in studying spectra of flares. He described the flash phase as the time at which a flare rapidly broadens into the wings of the H-alpha line. The term "explosive phase" was adopted by Moreton (1964) to describe the phase at which flares often show a marked increase in the rate of expansion at its borders in time-lapse filtergram observations. In the literature the terms "flash phase" and "explosive phase" are often used as if they are synonymous, assuming that the stage of rapid expansion in flare area (and brightness) is probably coincident with the rapid flaring in the wings of H-alpha. However, in this report, only the term explosive phase is used since the discussion concerns filtergrams and not spectra.

Figure 4 illustrates the development of a flare in the form of an integrated light curve of the flare as seen through a filter with a 1/2$\AA$ bandpass centered on H-alpha. The start of the flare is the point of first increase above the background intensity at the flare location. The start of the explosive phase is that point where a rapid change in flux occurs between the start and maximum of the flare. For our purposes we defined the start of the explosive phase as the intersection of the nearly straight line sections of the curve before and after the start of the explosive phase.

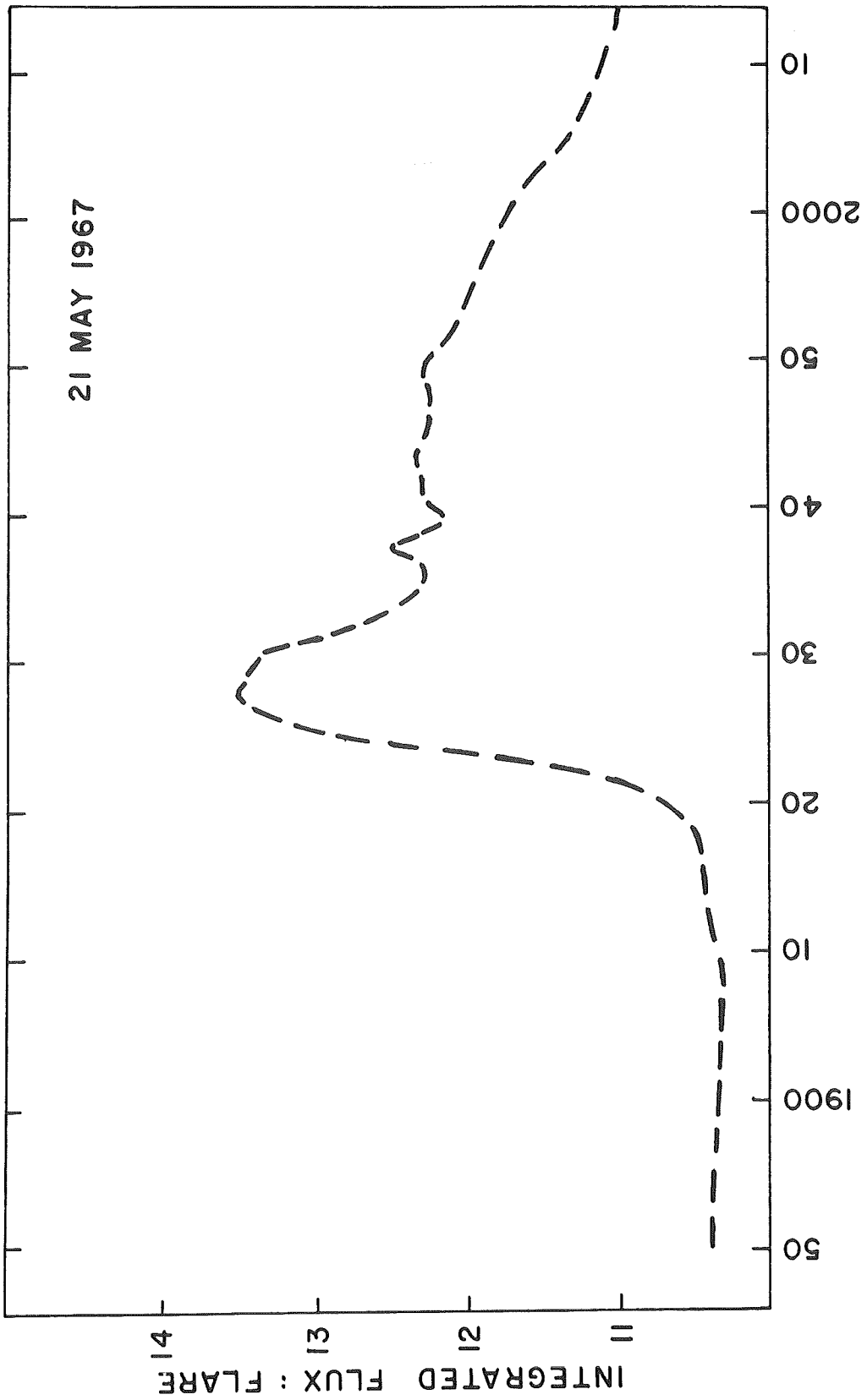


Figure 4. Integrated light curve of a flare as seen through a 1/2Å bandpass birefringent filter centered on H-alpha. The vertical axis is film density. The flare was composed of 4 distinct segments which result in the secondary maxima.

The curve in Figure 4 is the integrated H $\alpha$ flux from several flare segments each of which is probably an envelope of developing and decaying flare points. This should be kept in mind when comparing such curves with curves of radio and x-ray flux.

## 2.3 The Flare-Wave Phenomenon

Flare-associated waves have been referred to in the literature as "shock waves", "magnetohydrodynamic waves", "solar blast waves", "high speed disturbances" and "rapidly expanding features". When discussing the observational effects of this phenomenon, however, we prefer to simply refer to this kind of event as a "wave". At present we are still not certain whether or not we have directly observed this phenomenon which we call "wave". In most of the observations, we are only indirectly inferring the existence of a wave from the consistency and repeated occurrence of four types of observational effects associated with flares. These effects are 1) an abruptly initiated activation or oscillation of a filament outside the boundaries of a flare, 2) a front, interpreted as a depression and relaxation of the chromospheric fine structure, rapidly moving away from the active region of a flare, observed in the wings of H-alpha, 3) a very fast, bright, diffuse front of emission propagating away from a flare, usually only seen in the center of H-alpha, 4) progressive short-lived brightenings of small points of the chromosphere outside the active region of a flare.

Velocity is an important parameter in the interpretation of waves and the association of wave effects. However, the velocities which can be inferred from wave effects offer many sources of appreciable error because of the difficulty in determining the exact location and time of origin of waves and how long after the occurrence or passage of the wave-producing phenomenon each of the observed wave effects become visible.

Our most accurate measurements of velocity come from those events in which an absorption or emission front appears to propagate across the

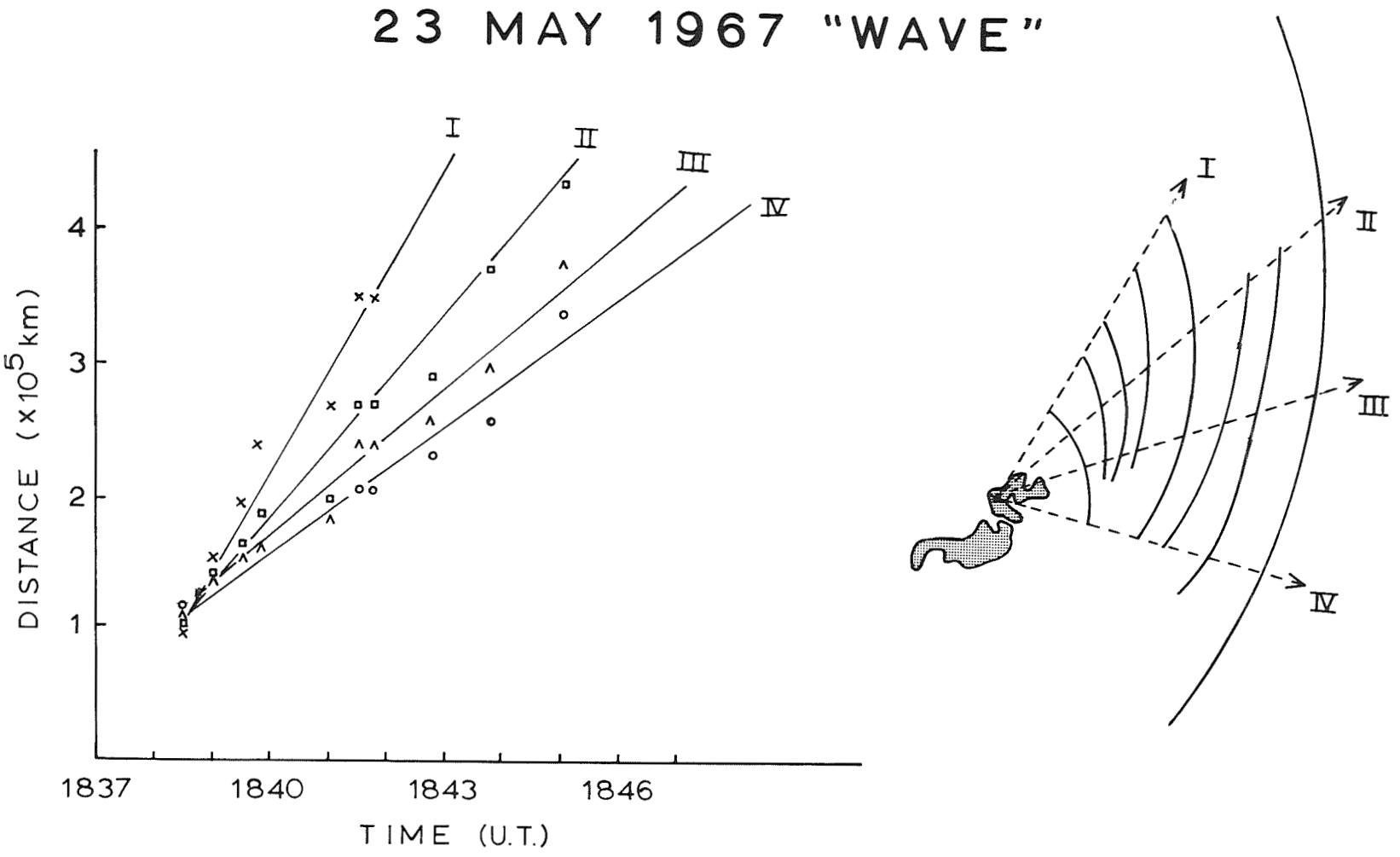


Figure 5. Diagram of the wave associated with the brightest flare on 23 May 1967. The measured velocity of the wave varies from 750 to 1125 Km across the wave front.

chromosphere outside the active region of the flare. Fourteen such cases existed in our sample of wave-effects associated with 57 flares.

An example of our method of determining the velocities of the 14 waves is shown in Figure 5. On the right is a diagram showing the apparent position of the wave on successive frames. By assuming a starting position at the flare, correcting for foreshortening, and plotting the position of the wave front on successive frames, we arrive at a velocity of propagation in the chromosphere. This example was selected especially because it does not show a uniform velocity across the wave front. The velocity varies from 750 to 1125 km per second across the wave front.

In many waves, excluding the one on 23 May 1967, the effects are only seen well outside the active region of the flare. Thus, the time of origin of the waves must be determined by extrapolating the velocity curve back to the time coordinate. The time origin of waves determined in this manner are compared in Figure 6 with the starting time of the associated flares. It is seen that for these 14 cases, the waves originated during the first 6 minutes of the flares. We then compare the time of origin of the 14 waves with the explosive phase of these flares as shown in Figure 7. It is immediately clear that 10 of the 14 waves originate within $\pm$ 30 sec. of the explosive phase. All of these waves originate within 2 minutes of the explosive phase. The cases in which the wave originates more than 30 seconds before or after the explosive phase are those cases in which the explosive phase could not be determined precisely. On the basis of this information, we are justified in using the explosive phase as the assumed time of initiation of waves for those cases in which the only visible effect is an oscillating filament or a chromospheric brightening. The velocities of waves which initiated clear cut oscillations and for which the explosive phase could be determined within $\pm$ 30 seconds cover the range of 410 to 2200 Km/sec. The mean velocity of waves producing filament oscillations, is 880 Km. per sec. The mean velocity of the 14 visible wave fronts is 710 Km/sec.

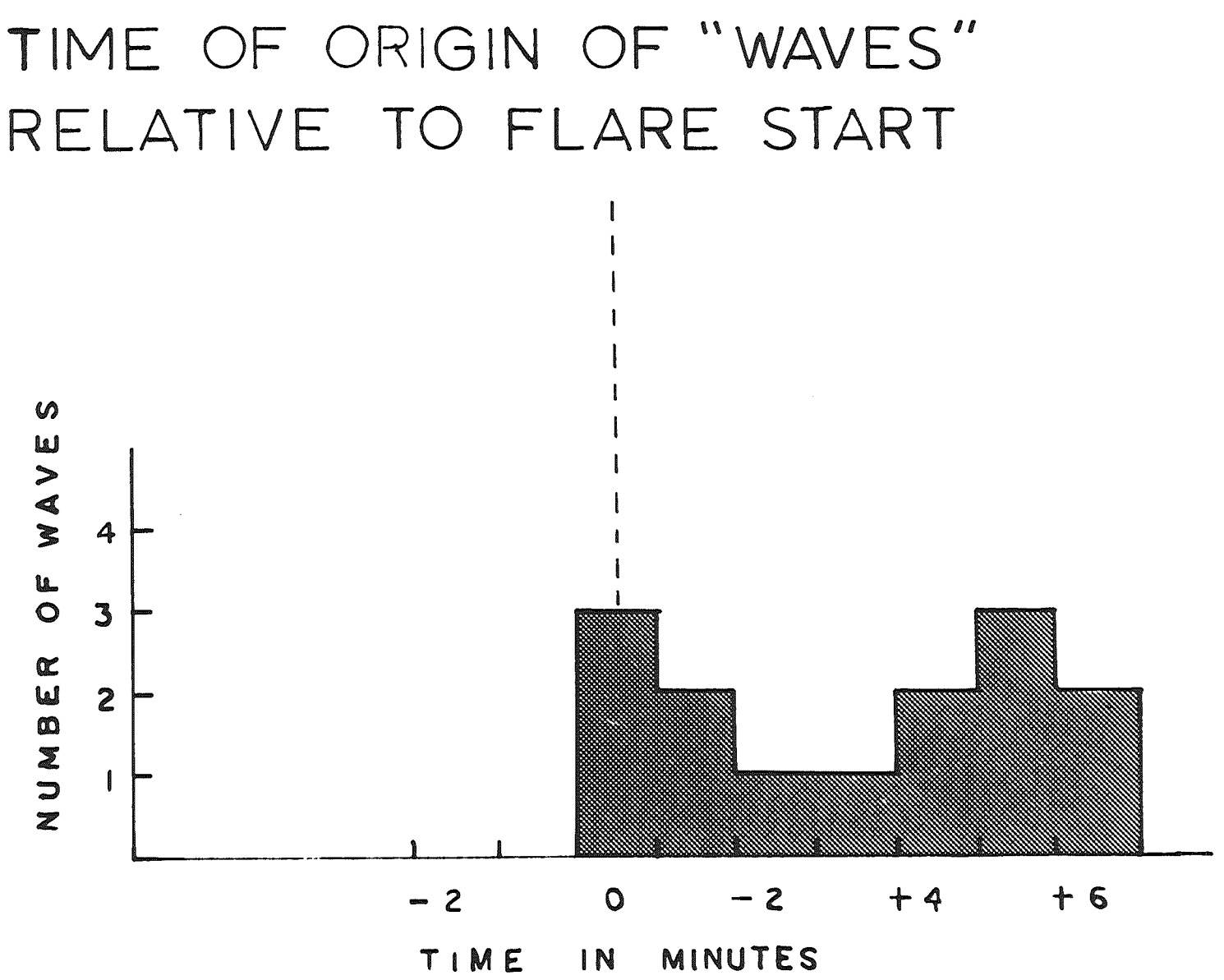


Figure 6. Histogram of the origin of waves relative to flare start for 14 events in which a wave front could be directly observed on H-alpha films.

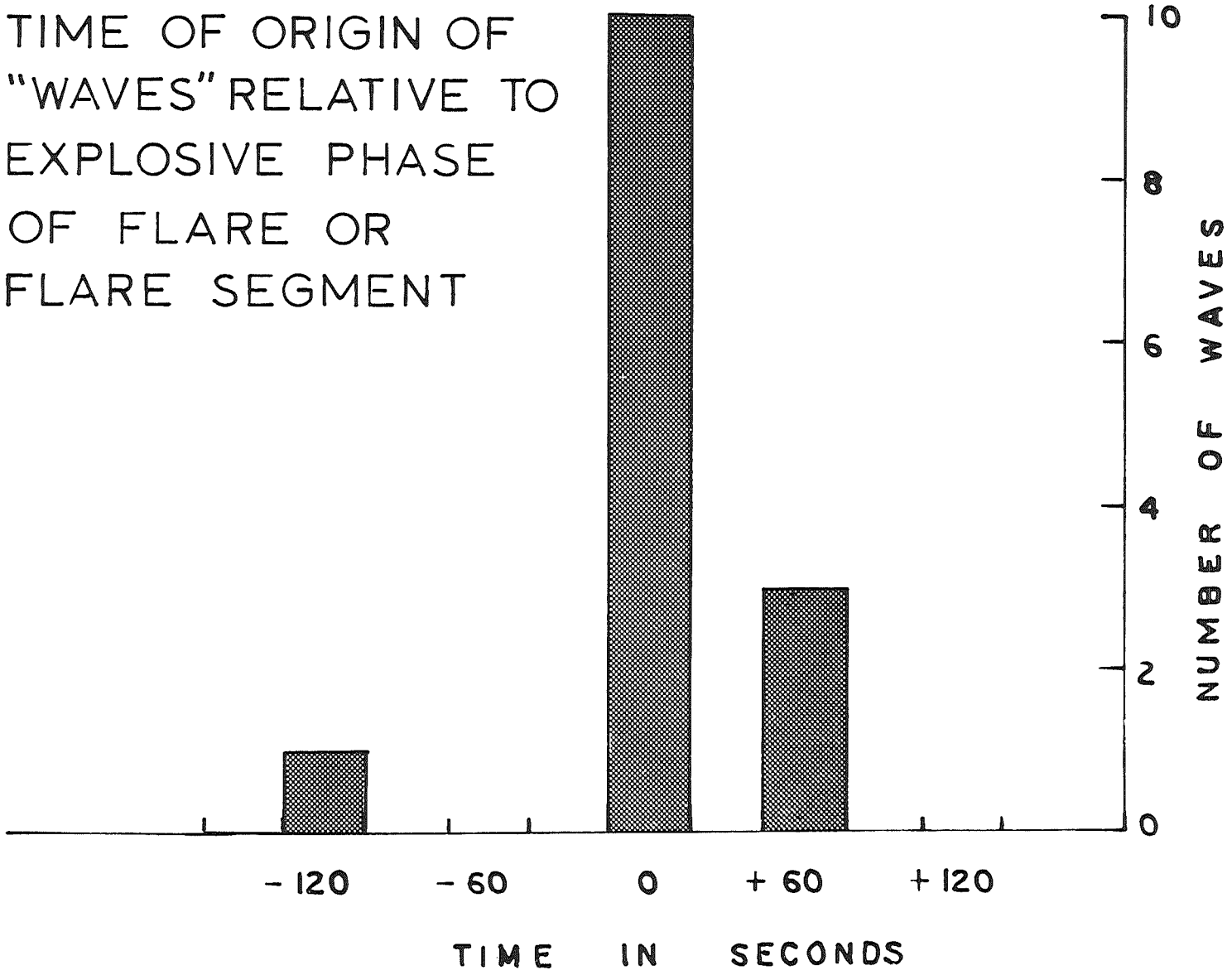


Figure 7. Histogram of the origin of waves relative to the flash phase or explosive phase of flares in 14 events in which a wave front could be seen on H-alpha films.

Another important feature of waves is that they seem to be highly directional. In most cases, the angular width of the observed effects is less than $90^{\circ}$. However, in several cases, effects were observed in opposite directions, that is, with a separation angle of nearly 180 degrees.

A diagram of the central direction of all the various wave effects is shown in Figure 8. The length of each arrow represents the mean velocity of each propagation. The solid lines are those effects for which velocity error is less than 30%. The dashed lines represent those cases in which a reasonable velocity could not be ascertained or the probable error was greater than 30%. The first feature to notice is that wave effects may occur in any direction from a flare. There is, however, in this sample a tendency for more wave effects to be observed to the south and west of the flare's position. Determining whether or not there is any physical significance in this preferential direction is a task beyond the scope of this study. We hope that more comparisons of these waves with Type II radio bursts, magnetic field maps, and with arrival times of particles observed in interplanetary space will shed more light on the nature of waves.

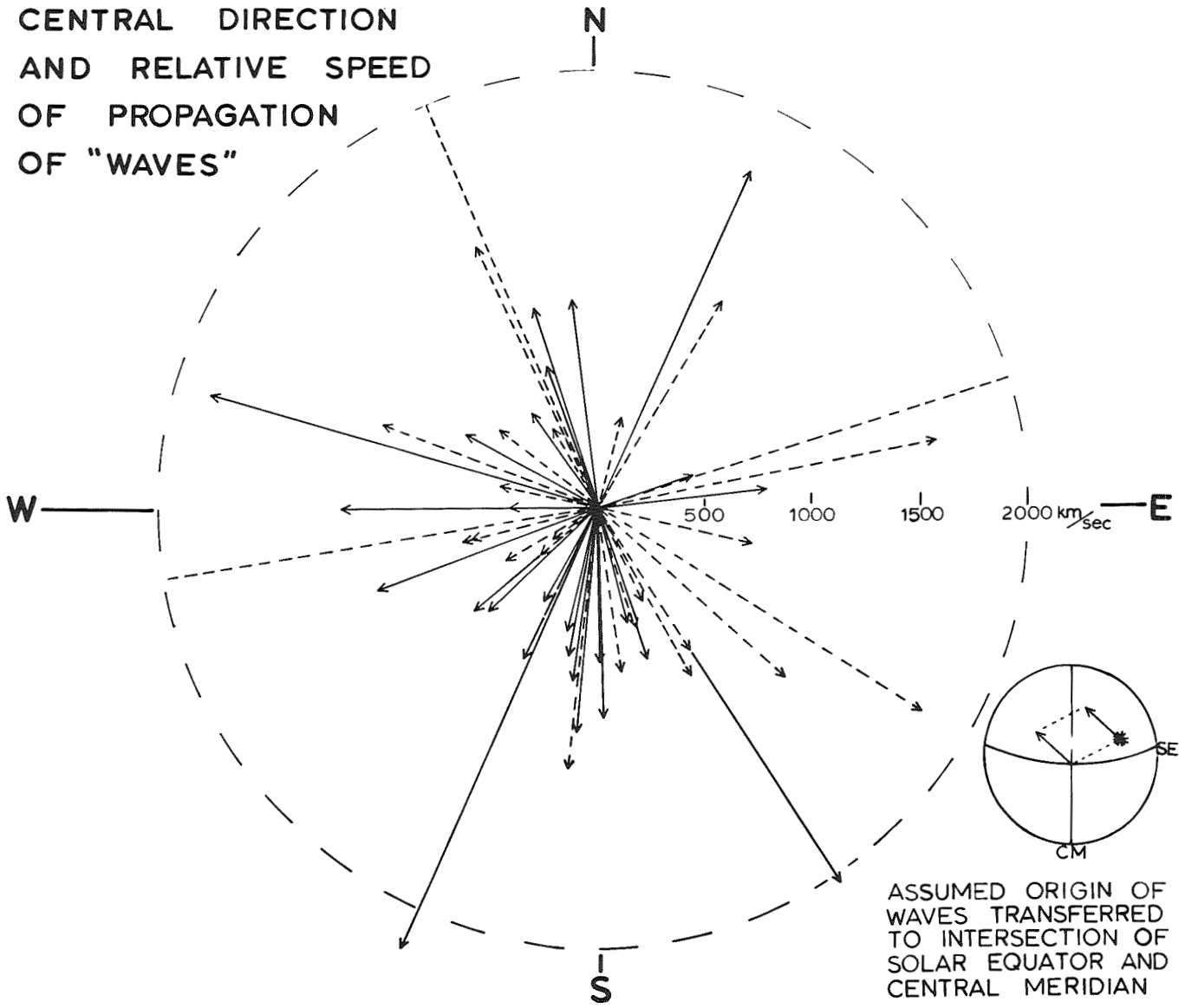


Figure 8. Central direction and velocities measured or inferred for 57 waves. Dashed lines represent events in which the velocity could be in error by more than 30%.

## Section 3

## X-RAYS, EUV EMISSION, RADIO BURSTS AND H-ALPHA FLUX CURVES OF SOLAR FLARES

### 3.1 Descriptions of Events

In this section, we are concerned with the relation of x-ray, EUV, centimeter radio emission, and some ionospheric effects to the H $\alpha$ flare. We have examined direct observations of x-rays and 10.7 cm radio bursts associated with the major flares starting at 1918 U.T. on 21 May 1967 and at 1758 U.T. on 23 May 1967. Ionospheric effects and EUV emission deduced from Sudden Frequency Deviation (SFD) data by Donnelly (private communication) has been compared with the 21 May flare and the major flare on 7 July 1966. Conclusions drawn from these comparisons are summarized in Section 3.2.

21 May 1967

The 21 May flare was the first major flare of many (flares) to occur in its active region. It is a reported proton and white-light flare. The start of the flare was preceded by a slow preflare brightening in the eventual-flare area. Flare start occurred at 1918 U.T. with a slow increase in H-alpha intensity. The start of the explosive phase was defined at 1921 U.T. with maximum occurring at 1927 U.T. During the decline of the main flare, a small section was observed to increase in brightness at 1932 U.T. The flare was composed of four definite flare sections.

Figure 9 shows the time history of the x-ray, H-alpha and EUV emission deduced from the associated Sudden Frequency Deviation, (Donnelly, private communication) for the 21 May 1967, 1918 U. T. flare. Both the hard ($< .6$ Å) and soft (2-12 Å) x-rays show a slow increase in intensity beginning around 1915 U.T., the approximate time of the first substantial

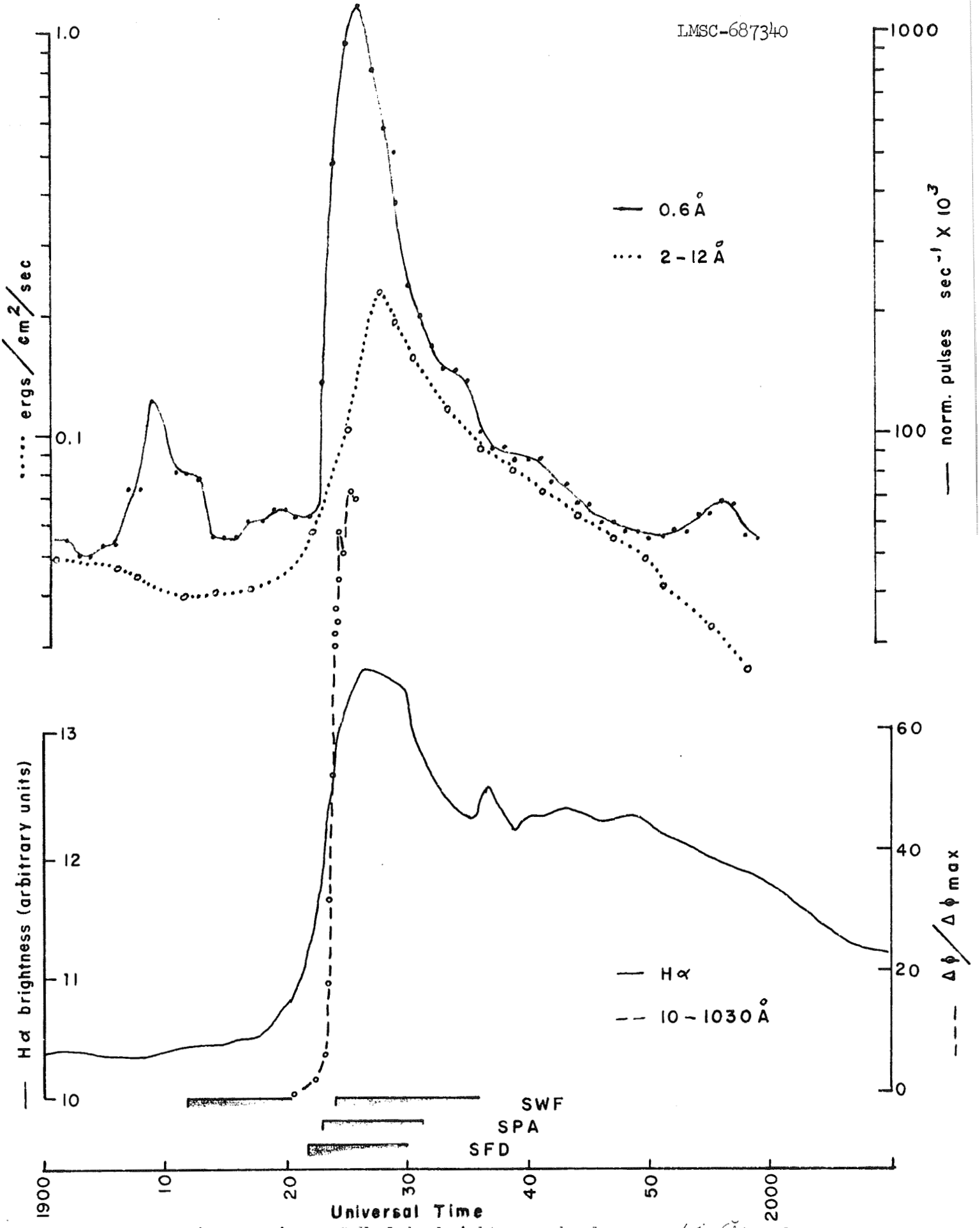


Figure 9. A comparison of H-alpha brightness, hard x-rays (< .6Å) and soft x-rays, (2-12Å) and EUV (10-1030Å) radiation for a flare on 21 May 1967.

increase in H-alpha flux. Van Allen (private communication) defines the significant increase in the 2 - 12Å flux as beginning at 1921 U. T. This time corresponds (within one minute) to the start of the explosive phase of the 21 May flare. The soft x-rays closely resemble the H-alpha flare. The hard x-rays, however, were delayed by two minutes, beginning with an abrupt increase at 1923 U.T. The hard x-ray peak precedes the H-alpha flare and soft x-ray maxima by 1 minute. The 10 - 1030Å flux, deduced from the ionospheric SFD data by Donnelly, begins increasing at 1920.8, near the onset of the explosive phase. Peak flux is reached at 1925.7 or slightly after. The observed ionospheric effects are indicated by bars in Figure 9. The flare-associated D region effects (SWF and SPA) began between 1923 and 1924 U. T. though an SWF was reported at 1912 U.T. The maximum of the D region effects occurs at 1932 U.T. The SWF at 1912 U.T. is probably related to the slow increase in hard and soft x-rays observed at that time. The E and F regions were effected early in the flare's development and slightly before the major D region effects were observed. The D region disturbance began at 1923 U.T. coincident in time with the onset of hard x-rays and during the most rapid increase in the soft x-ray and EUV flux.

23 May 1967

On 23 May 1967, three importance 2B flares occurred in succession beginning around 1800 U.T. The first and least complicated of the three flares will be considered here. The H-alpha flux curve of the flare, the time histories of the hard x-rays (< .6Å Winckler, 1968) and soft x-rays (2 - 12Å Drake et al. 1968) and the 10.7cm radio flux (Erickson, 1968) are shown in Figure 10 and are summarized in Table 1.

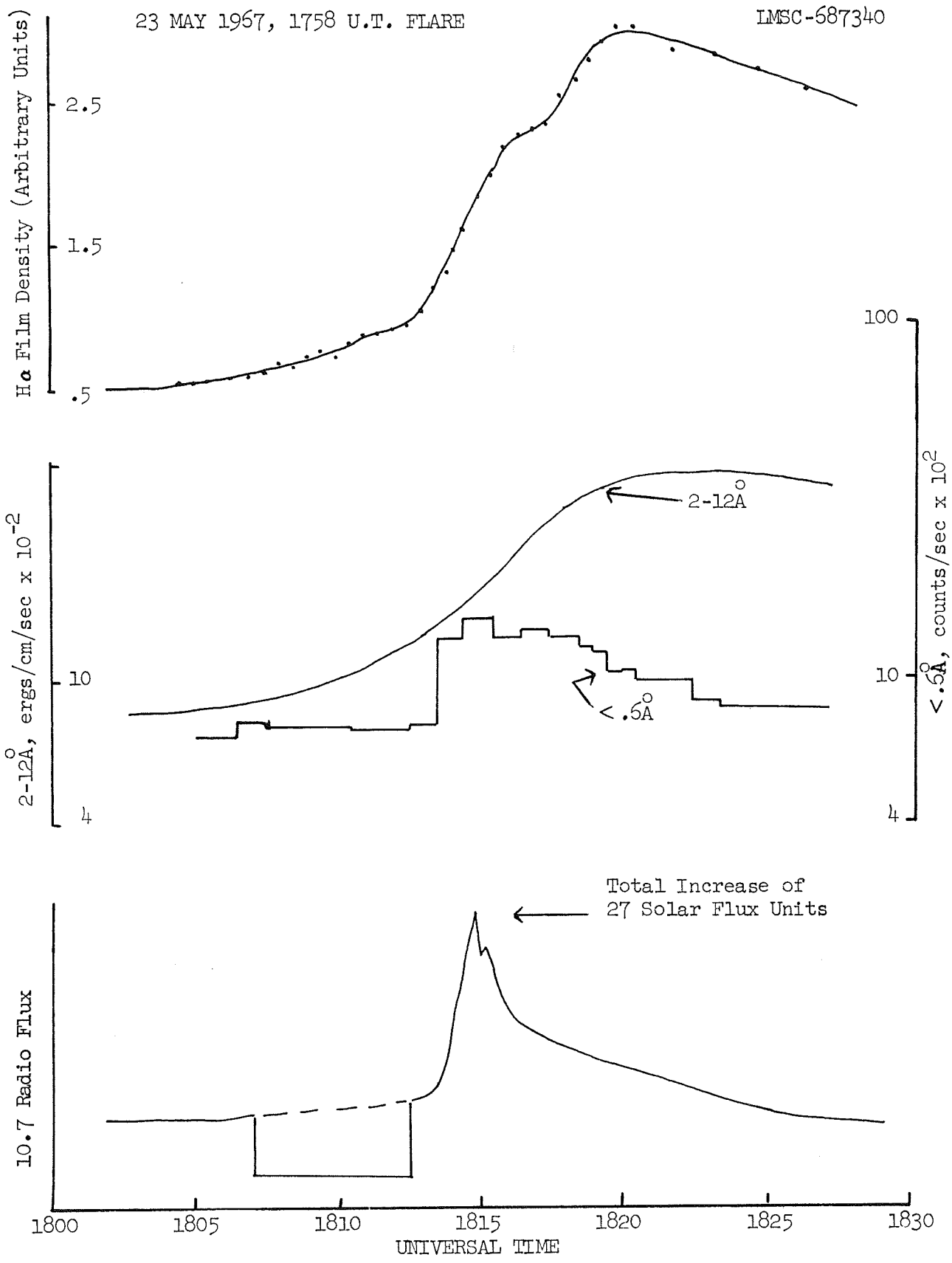


Figure 10. A comparison of x-ray, radio and H-alpha light curves for the event of 23 May 1967. Hard x-rays show a similarity in time profile to the radio event.

TABLE 1

| | Start | Start of Explosive-Phase | Maximum | Source of Data |
|---|---|---|---|---|
| Flare | 1758 U. T. | 1808:00 U. T. | 1815-17 U.T. | Angle 1968 |
| 10.7cm burst | 1800 | 1808 | 1809:40 | Erickson 1968 |
| X-ray burst 6Å | 1808 | | 1810 | Winckler 1968 |
| 2 - 12Å | 1759 | | 1817 | Drake et al |

The 23 May flare started at 1758 U.T. and was preceded by an increase in plage intensity in the potential-flare area resulting from the occurrence of several small brightenings in the 40 minutes prior to flare onset. When the flare began at 1758 U.T., an increase in H-alpha intensity simultaneously appeared in three separate areas of plage. The start of the explosive phase was defined at 1808:00 U.T. Flare maximum was reached at 1815 U.T. with the flare intensity beginning to decrease by 1817 U.T.

Coincident with the start of the flare, the 10.7cm radio flux showed a slow increase beginning around 1758 U. T. A more dramatic increase began at 1808 U. T. coincident with the start of the explosive phase of the flare. Peak flux was reached at 1809 U.T.

A definite rise in the 2 - 12Å flux was observed around 1730 U.T. at the time of the preflare increases in plage intensity. The hard x-rays ($< .6$Å) do not show the same increase, but at 1752 U.T. the hard x-rays begin increasing steadily. From 1756 U.T., the 2 - 12Å data also show a steady increase in flux. The 2 - 12Å x-rays show a smooth increase in flux to a maximum at 1817 U.T., while the x-rays of $< .6$Å abruptly increase at 1808 U. T. with the peak flux occurring at 1810 U.T. The $< .6$Å x-ray flux decreases fairly rapidly reaching nearly their preflare value before the onset of the second flare. The 2 - 12Å x-rays show a slower decline.

7 July 1966

The 7 July 1966 flare occurred in a rapidly developing region and is a reported proton flare. The first visible increase in H-alpha occurred at 0023 U. T. The flare was composed of two flare sections (Angle 1968) which developed somewhat independently of each other. The maximum of one flare section was reached fairly rapidly at 0030 U. T. and the second flare section developing less rapidly with maximum occurring at 0045 U.T.

A schematic of the H-alpha flare intensity variations and of the observed 2 - 12Å x-ray variations are shown in Figure 11. Van Allen (1967) reported that the increase of x-ray intensity to maximum for the 7 July 1967 flares was a composite of three phases: (1) a slow increase in flux from 0023 to 0026 U.T., (2) a rapid increase from 0026 to 0030 U.T. and a leveling off to about 0035 U.T., and (3) another increase in x-ray flux from 0035 U.T. reaching a maximum at 0042 U.T. The < .6Å x-rays (Arnoldy et al. 1968) show a time variation similar to the 2 - 12Å x-rays. The hard x-rays begin increasing at 0025:30 U.T. reaching the first maximum at 0031 U.T. After a slight decrease, the flux again increased to the second maximum at 0038 U.T. Richmond (1968) found that the sfe (solar flare effect) occurring with the 7 July flare had two peaks, the first at 0029.5 U.T. (3 minutes after the start of the sfe) and the second at 0045 U.T.

Along with this observation, we note that the observations of the SCNA indicate that the D region went through two increases in ionization with a maximum around 0033 and 0040 U.T. This would indicate that the 0 - 10Å flux began increasing rapidly at 0026 U.T. reaching its first maximum at 0030 - 0033 U.T. and its second maximum between 0040 and 0045 U.T.

The SFD associated with this flare has been analyzed by Donnelly (1967). The calculated 10 - 1030Å radiation was found to show the same double peak as observed in the 0 - 10Å range. The 10 - 1030Å radiation began increasing at 0026 U.T. peaking at 0029 U.T. The radiation began in-

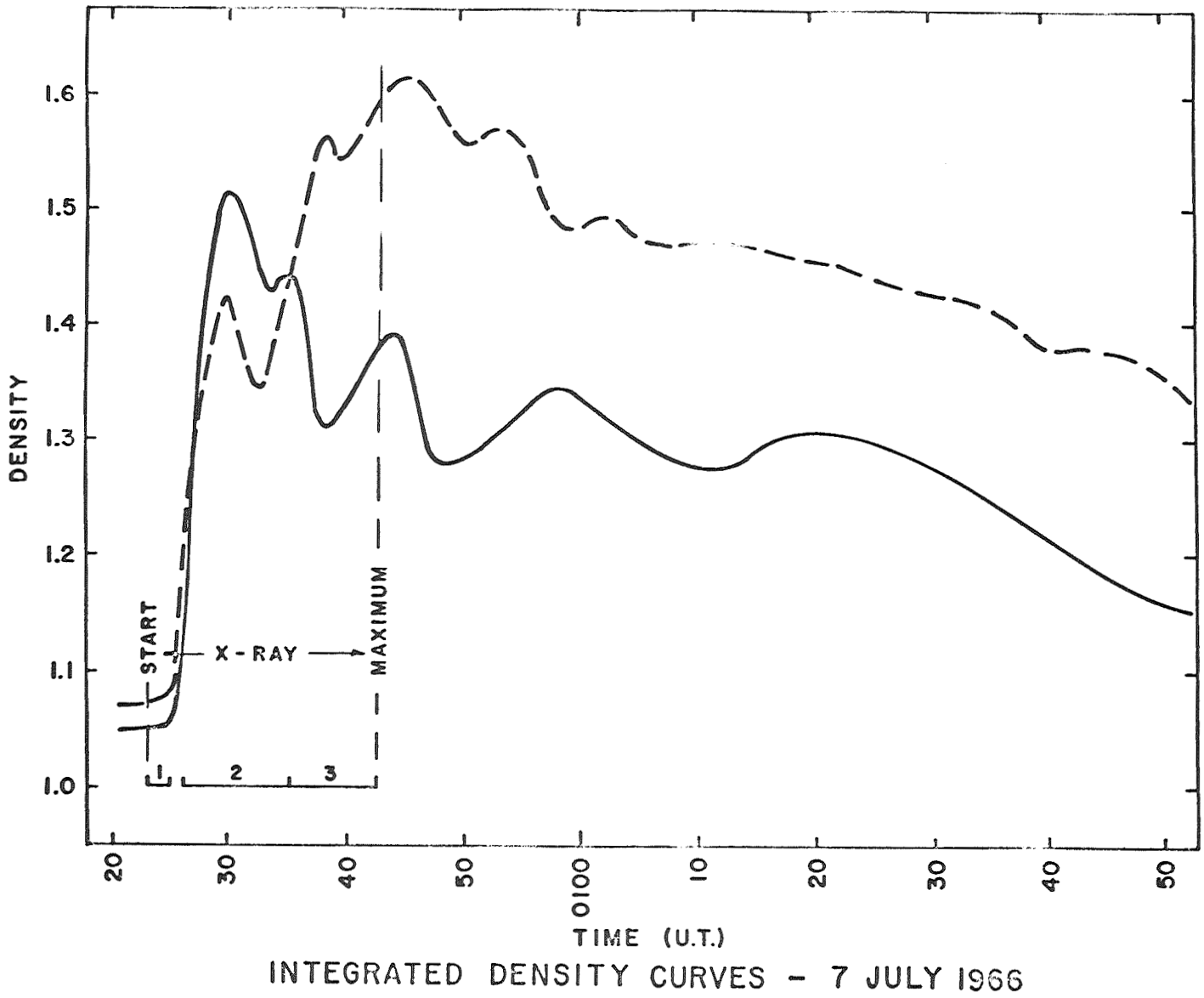


Figure 11. An H-alpha light curve of two segments of a flare compared to 3 phases in the associated x-ray event.

creasing again at 0035 U.T. reaching its second maximum at 0038 U.T. The 10 - 1030A flux remained fairly constant until 0042 U.T. at which point it began decreasing slowly.

The 7 July 1966 flare was composed of two flare sections which developed semi-independently. The ionizing radiation (as deduced from ionospheric disturbances and observed directly) showed two fluctuations which in time were related to the individual behavior of the two flare sections. The observed ionospheric effects in the D region began with an abrupt increase of the 2 - 12A x-ray radiation and at the time the spectrum of the flare was hardening.

3.2 Conclusions From The Study of Selected Events*

Based on the above examples, we can make the following tentative conclusions:

1) In general, there is a good correspondence between the time history of the H-alpha flare and the 2 - 12A x-ray flux. These soft x-rays have a smooth rise in flux and seem to follow the characteristics of the H $\alpha$ flare relatively closely, e.g. time of start, flash phase and maximum. In the case where a poor relationship was found, the flare had an associated bright surge which biased the interpretation of the H-alpha flux curve.

2) The hard x-rays (less than .6A) show an abrupt increase from 0 to 2 minutes after the start of the H-alpha explosive-phase, peak prior to H-alpha flare maximum, and coincide with the maximum of the 10.7cm radio burst.

3) The EUV emissions, deduced from the Sudden Frequency Deviations (SFD-

---

* The information in Sections 3.1 and 3.2 were prepared by Karen L. Angle as part of her thesis on Ionospheric Effects of Solar Flares.

E and F ionospheric effect, Donnelly, 1969), began at the onset of the explosive phase. No exceptions were found to this observation. EUV peak flux was reached prior to H-alpha maximum and usually near the time of the observed peak in hard x-rays and in the radio bursts at 3000 MHz.

4) The start of the reported 10.7cm radio flux or of an abrupt increase in 10.7cm radio flux (as in the 1758 U.T. 23 May 1967 flare), is concurrent with the start of the explosive-phase of the flares. However, in examining the records, small increases at 10.7cm can be detected coincident with the start of the flare.

### 3.3 Very Small Flares With Radio Bursts and X-rays

Numerous tiny flares are observable in the Lockheed large-scale H-alpha films which are not readily distinguishable on the flare patrol films and consequently are not included in the lists of flares published by ESSA. For example, in the very large complex region (McMath Plage No. 8942) which was visible on the solar disk from 19 - 30 August 1967, 5 importance 1 flares and 43 subflares were reported by Lockheed from the flare patrol films. In the large scale films, however, well over 100 distinct subflares can be seen. Since few flares occurred in other regions during this time, this region seemed suitable for trying to determine if there is a minimum size or type of flare for which 2700 or 2800 MHz radio bursts are not recorded.

From the large-scale films, a list was made of the 114 most obvious subflares in this region. 2800 MHz radio observations were made at the Algonquin Radio Observatory (Ottawa) during 105 of these 114 subflares and during 4 of the 5 importance 1 flares. Out of these 109 events, clear 2800 MHz radio bursts were observed for 100% of the 6 flares having areas $\geq$ 1.5 square degrees, for 58% of the 12 flares having areas between 0.7 and 1.4 square degrees, for 16% of the 19 flares having areas between

0.3 and 0.8 square degrees, and for 14% of the 72 subflares which were not reported. 26% of the unreported subflares and 16% of the flares $\bar{<}$ 1.5 square degrees were associated with tiny questionable bursts while for the remainder of the flares there was no evidence of even a weak burst. The distribution of these flares by area and brightness is shown in Table 2.

In surveying the films subflare brightness did not seem to be a consistent indicator of the presence or absence of an associated radio burst. This observation was checked by comparing the occurrence of associated radio bursts with only those 36 subflares which were tabulated in the flare reports. Flare intensities were reported as faint, normal, or bright on the basis of visual estimates.

Using the same area divisions it was found that 100% of these reported flares with areas $\bar{>}$ 1.5 square degrees were of normal or greater brightness, that 50% of these flares with areas between 0.9 and 1.4 square degrees were of normal brightness, and that only 10% of the flares having areas less than 0.8 square degrees were of normal brightness; the remainder in all categories being classed as faint. Thus, a positive correlation between subflare brightness and subflare area exists in this data. Visual estimates of flare brightness cannot be considered an independent parameter as far as subflares are concerned. Photometric measurements might yield a different result.

The question remains whether brightness is as good a criteria for determining association with radio bursts as flare area. For the normal intensity flares having areas $\bar{>}$ 0.9 and < 1.5 square degrees, 6 of 9 (66%) were definitely associated with radio bursts and for the faint intensity flares having areas < 0.9 square degrees, 3 of 21 (16%) were definitely associated with radio bursts. From these numbers, it is apparent that about the same relationship exists between burst occurrence and subflare brightness as between burst occurrence and subflare area. Therefore, essentially no gain is made by using visual estimates of brightness

TABLE 2

| | FLARE AREA (Sq. Deg.) | | | | |
|---|---|---|---|---|---|
| 2700/2800 MHz Association (Flare Intensity) | No Report | .3 - .8 | .9 - 1.4 | $\bar{>}$ 1.5 | Total Events |
| Definite Burst (Bright) | 10 | 3 (0) | 7 (0) | 6 (1) | 26 (1) |
| Questionable Burst (Normal) | 19 | 3 (2) | 2 (7) | 0 (5) | 24 (14) |
| No Burst (Faint) | 43 | 13 (18) | 3 (4) | 0 (0) | 60 (22) |
| Total Events | 72 | 19 (20) | 12 (11) | 6 (6) | 109 (35) |

TABLE 3

| | FLARE AREA (Sq. Deg.) | | | | |
|---|---|---|---|---|---|
| x-ray Association | No Report | .3 - .8 | .9 - 1.4 | $\bar{>}$ 1.5 | Total Events |
| Definite x-ray Event | 5 | 5 | 2 | 4 | 16 |
| Questionable x-ray Event | 11 | 6 | 3 | 1 | 21 |
| No x-ray event | 12 | 5 | 3 | 0 | 20 |
| Total Events | 28 | 16 | 8 | 5 | 57 |

instead of measured area for determining the probability of the occurrence of a definite radio burst. Using either area or brightness or both, one has, at best, a 70% chance of correctly guessing whether or not a radio burst would or would not occur using the categories discussed for this data.

The large-scale films were carefully surveyed to see if there were any possible characteristics, other than flare importance (brightness and area), which might be associated with the occurrence or non-occurrence 2700 or 2800 MHz bursts. It was noted that on a given day the subflares associated either with or without radio bursts could occur in the same locations within the active region. The larger and brighter flares were the ones associated with bursts in a given location. Thus, there appears to be no evidence that the configuration of polarities in the magnetic field, to which the flares relate, could in any way affect the occurrence or non-occurrence of a radio burst.

In surveying the films, however, it did seem that the abruptness of the start of a subflare or its rate of rise to maximum intensity could be related to the occurrence or non-occurrence of radio bursts. For the 24 subflares and unreported flares with definite radio bursts, the time between flare start and maximum intensity was taken as a measure of the rate of rise to maximum without regard to the areas of these flares. Comparing these rise times with the appearance of the associated radio bursts revealed that the subflares with the rapid rise times corresponded to the radio bursts with the sharpest onsets and that the subflares with the slowest rise times were the most difficult to identify in the radio records. In Figure 12 the radio bursts are presented in order from those whose associated subflares have the shortest rise times to those which have the longest rise times. There is a marked change in the character of the radio bursts corresponding to the increasing rise times of the associated subflares. The bursts associated with subflares having rise times of 5 or less minutes (left side, Figure 12) have very abrupt onsets, very short lifetimes and are readily identifiable even though the

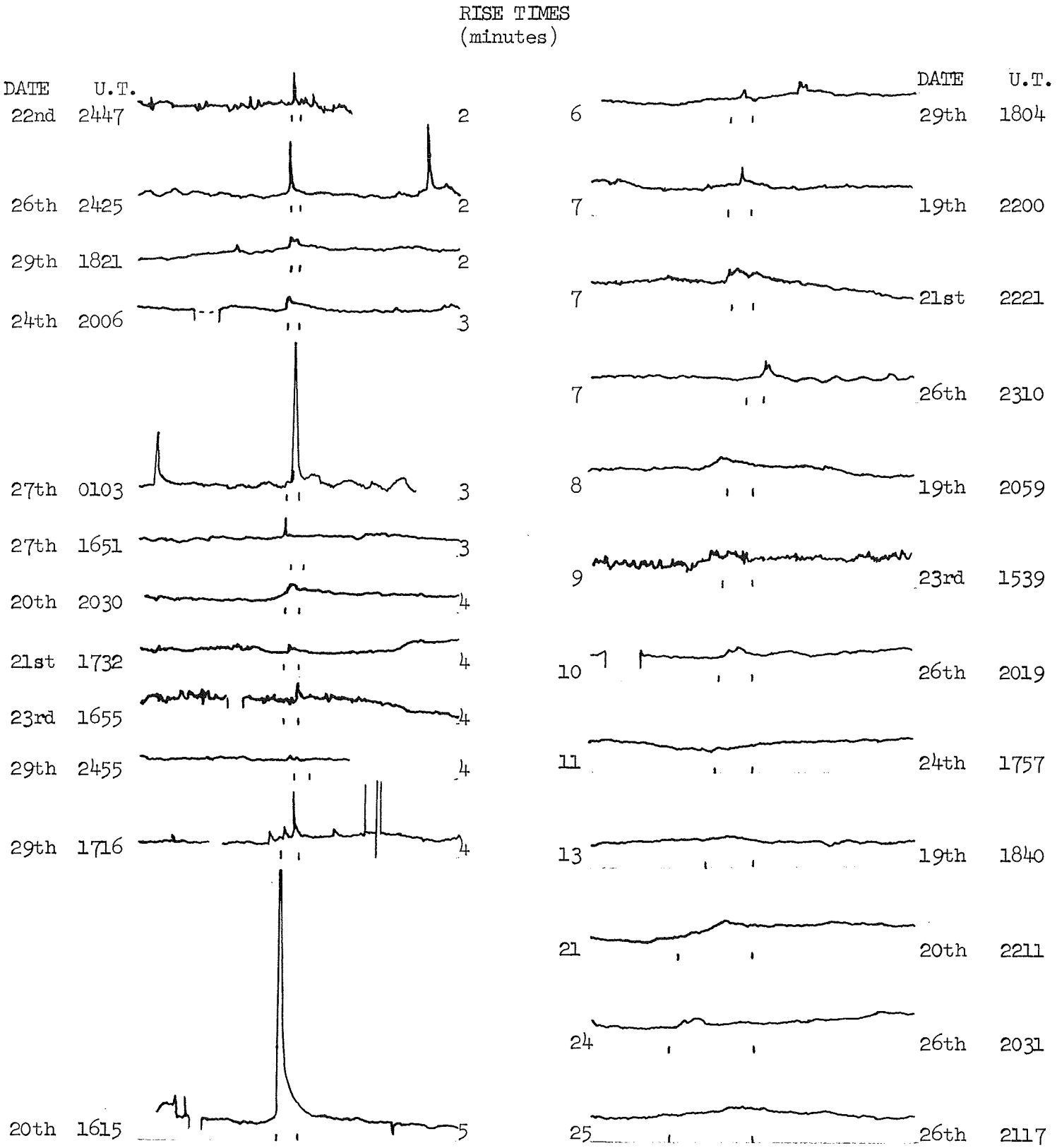


FIGURE 12. 2800 MHz radio bursts recorded at the Algonquin Radio Observatory (Ottawa) are shown corresponding to subflares and unreported flares which occurred in McMath Plage 8942 from 19 to 30 August 1967 during observing hours of the Lockheed Solar Observatory. The bursts are shown in order of increasing rise times of the associated flares (flare maximum-flare start). The subflares and unreported flares with long rise times(> 10 min.)may not be reported as radio bursts since they appear only as slight increases in the radio signal.

amplitude of the burst may be very low. The bursts associated with subflares and unreported having rise times between 6 and 10 minutes have much less distance onsets and are recognizable as bursts of longer duration often with one or more low amplitude peaks superposed on a slight rise in the radio signal. The bursts associated with subflares and unreported flares having rise times longer than 10 minutes are recognizable only as long slow increases which are scarcely distinguishable from the background signal. From this illustration one can surmise that tiny flares without either an abrupt start or an abrupt increase after the start of the flare would probably not be identifiable as radio features which would stand out against the background signal. However, if radio data at this frequency were available with spatial resolution on the order of a few minutes of arc, many more subflares would probably be identifiable as radio flares. Conversely, if high resolution H-alpha observations were available for the whole disk and limb, it is highly doubtful that solar radio bursts would be observed without corresponding optical flares.

It is evident that the radio signal of a flare is closely related to the individual character of the flare as seen in H-alpha. This means that the lack of correlation which has recently been stressed between optical reports of flare importance and reports of radio events is due primarily to inadequate means of measuring the optical characteristics of flares and not to any real identifiable differences in the energy spectra of flares at optical and radio wavelengths.

X-ray data from the OGO IV satellite was made available for this study by R. Kreplin of the Naval Research Laboratory. This data was suitable for the study of small events since the x-ray flux from each of 4 channels, 0.5 - 3Å, 1 - 8Å, 8 - 20Å and 44 - 60Å, are plotted at 30 second intervals. Of the 119 flares in region 8942, 42 occurred when the OGO IV satellite was recording data and at such times when the OGO IV satellite was not in the shadow of the earth or when particle events totally eliminated the possibility of ascertaining whether or not solar x-ray events were occurring.

The occurrence of x-ray events could also be established for an additional 15 small flares appearing in other regions during the same period, making a total sample of 57 events. In Table 3 these 57 flares are grouped by reported areas and their association with x-ray events. It is seen that 4 of the 5 flares with areas $\geq$ 1.5 square degrees are definitely associated with x-rays while 1 was associated with a questionable x-ray event. Only about 30% of the flares with areas between .3 and 1.4 square degrees are definitely associated with x-rays. 18% of 28 flares which were not reported were also x-ray events. Comparing these numbers with those in Table 2, it is evident that the fraction of flares in these groupings that are associated with x-rays is not appreciable different than the fraction associated with radio bursts. The fraction of definite associations agree within 20% which is relatively close for such a small sample of events.

In Table 3 it is seen that only 16 of these 57 flares were definite and unambiguous x-ray events. 8 of the 16 were also confirmed radio events at 2800 MHz. 3 were questionable radio events, 3 could not be identified with any radio event and for 2, no radio data was available. All of the x-ray flares above 1.5 square degrees and all except 2 above 1.0 square degrees were also radio events, assuming the availability of radio data. For the unreported flares with areas $<$ 1.0 square degrees but which were associated with x-ray events slightly less than half were also confirmed as radio events.

Conversely in the radio data, of the 25 definite radio events, unambiguous x-ray data was available for only 10. As stated above, 7 were definite x-ray events. 2 were associated with questionable x-ray events while for only 1 radio event, no x-ray event could be seen.

Thus, if one observes either a definite radio burst or a definite x-ray event, there is about a $\geq$ 70% chance that it will also be associated with the other. For flares $\geq$ 1.5 square degrees, the chance of mutual assoc-

iations of radio bursts and x-ray events, given one or the other, is nearly 100%. For subflares < 1.5 square degrees, the chance of mutual association of x-rays and radio bursts at these frequencies is around 50%.

In the current day flare-prediction and flare reporting activities, there is occasional need for being aware of the occurrence of subflares < 1.5 square degrees. However, for the sake of practicality, one can conclude that either sensitive x-ray or radio monitors can adequately record the occurrence of most significant flares if interference from other sources does not prohibit the detection of solar events.

# Section 4

# SOME RADIO BURSTS AND THEIR RELATION TO CHARACTERISTICS OF H-ALPHA FLARES

## 4.1 Post Burst Increases at Decimeter Wavelengths

During the maximum and decay of flares, sporadic radio bursts sometimes occur which apparently have no counterpart in soft x-rays. Because of the close correspondence between light curves of flares and soft x-rays, the absence of x-rays corresponding to the late burst increases leads one to suspect that these radio signals may be associated with some aspects of flares other than the bright emission at optical wavelengths. In H-alpha observations, there are several types of dynamic features associated with flares which may be directly related to late burst increases in radio events. Three possibilities are loops, surges, and prominence material falling onto the disk. An example of a loop system and a surge are discussed and illustrated as possible candidates for optical counterparts to some post burst increases.

In a discussion of the Sagamore Hill Radio Observatory observations of the flare of 28 August 1966, Castelli and Michael (1967) have pointed out that the post burst increases show increasing intensity and activity proceeding from higher to lower frequencies a pattern not shown by the initial burst (Figure 13). In H-alpha, a system of loops became obvious a few minutes after the primary maximum of the flare, and as early as 1540 U.T. (Dodson and Hedeman 1968. These loops are readily seen in Figure 13 as narrow, bright threads extending from one segment of the flare to the other. As the flare decays some of the loops appear in absorption instead of emission against the solar disk. There are several reasons for suggesting that these loops may be the optical counterpart of the post-burst increases at decimeter wavelengths. First, they coincide in time. Second, the development of such loops, when more typically seen on the limb, is somewhat sporadic as also are the post burst increases. Third, loops

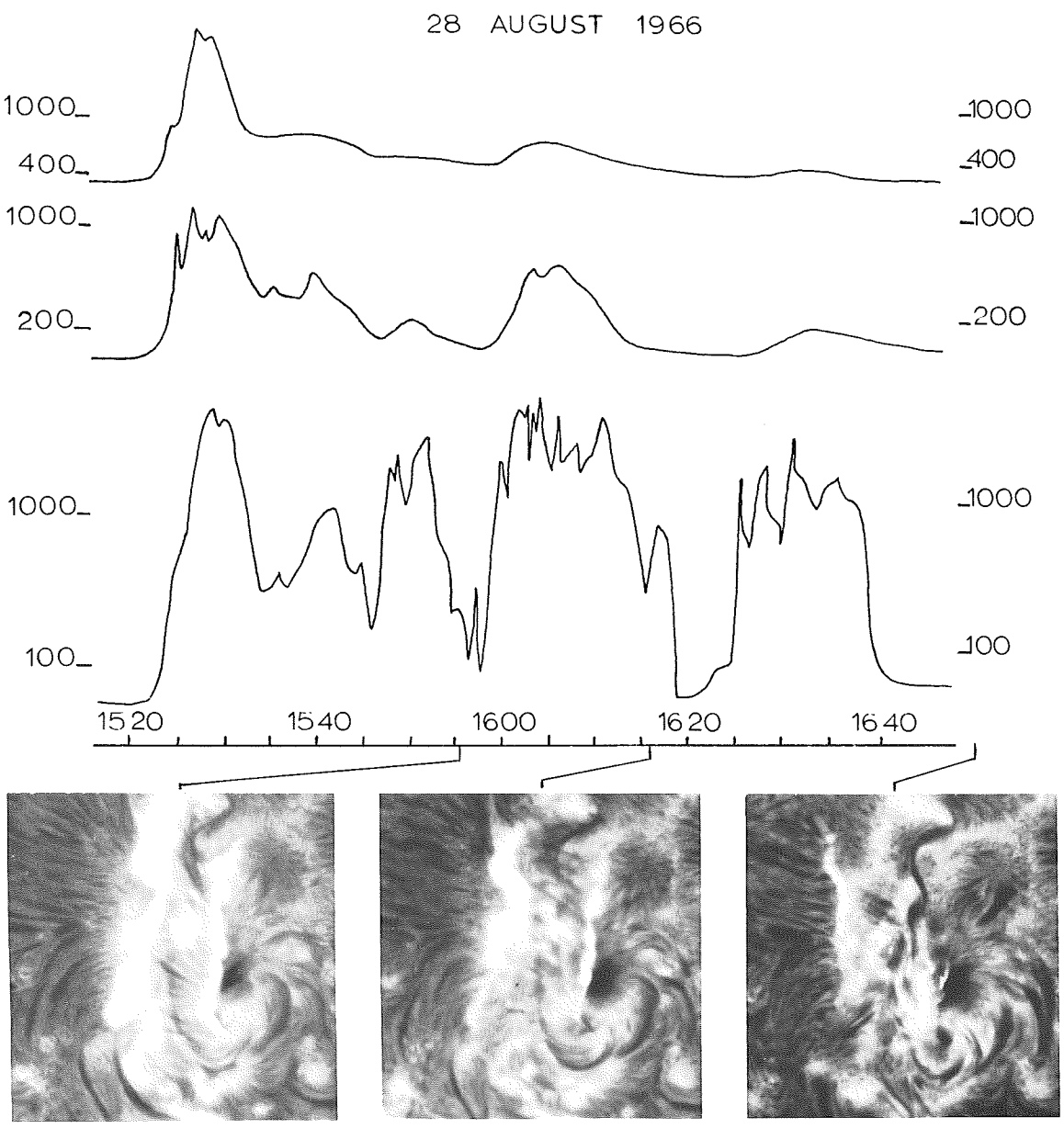


Figure 13. A comparison of the tops of flare loops between the 2 flare segments is made with the post burst increases in the event on 28 August 1966.

initially form from condensations of material in the corona above flares with subsequent down flow of material along both ends of the loops. This characteristic may be associated with the increased intensity and structure in the radio signal proceeding from higher to lower frequencies. Lastly, in this event, there is no other optical phenomenon which also could be identified with the burst increases late in the flare.

Another example of a post burst increase after the initial burst with the development of a flare is shown in Figure 14 for an event on 21 May 1967. Although there is some increase in structure at the lower frequencies, this event differs from the 28 August 1966 event in that the relative intensity of the late burst to the initial burst does not increase toward lower frequencies. In this event, we suggest that the late burst may be associated with the unusual fan-shaped structure depicted in Figure 15 which will henceforth be referred to as a fan surge or surge although it is not typical of events usually known as surges. The fan-surge begins to develop at around 1930 U.T. coincident with the start of the late burst increases. The burst continues until about 1950 U.T. when the surge has nearly vanished. Between 1934 and 1940 U.T. the surge attains its maximum density and spreads out into the shape of a fan. During this short interval the late burst also develops and reaches a maximum at 1938 U.T. Around 1934 U.T. the surge appears to change from an emission feature with a dark base to an absorption feature with a base of emission in the center of H-alpha. In the wings of H-alpha, however, the surge appears as an absorption feature throughout its lifetime. In addition to coincidence in time, two other factors suggest that the fan surge should be identified with this post burst increase. The intensity of the burst decreases with decreasing frequency, consistent with the idea that the stronger signal may be coming from the more dense base of the surge than from the fingers spreading and extending into the corona. Also, as one can see in Figure 15, there is evidently no loops or other structure with which to associate this later burst, unless it could possibly result from additional development of the flare.

MAY 1967

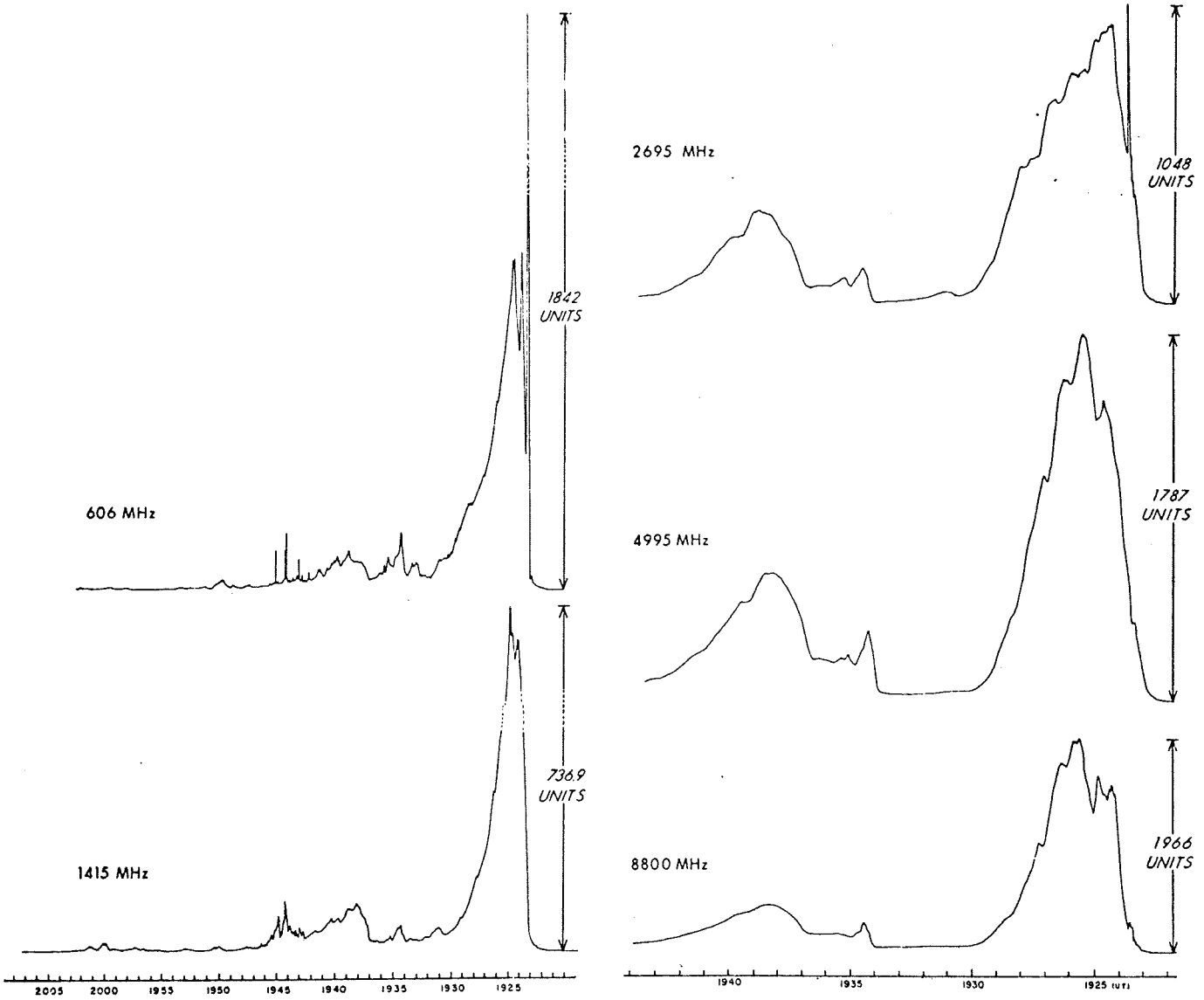


COMPLEX RADIO BURST OBSERVED ON 21 MAY, 1967 AT SAGAMORE HILL RADIO OBSERVATORY (AFCRL) HAMILTON, MASS.

Figure 14. This event is shown for comparison of the late burst increase from 1934 to 1950 with the fan-shaped surge in Figure 15.

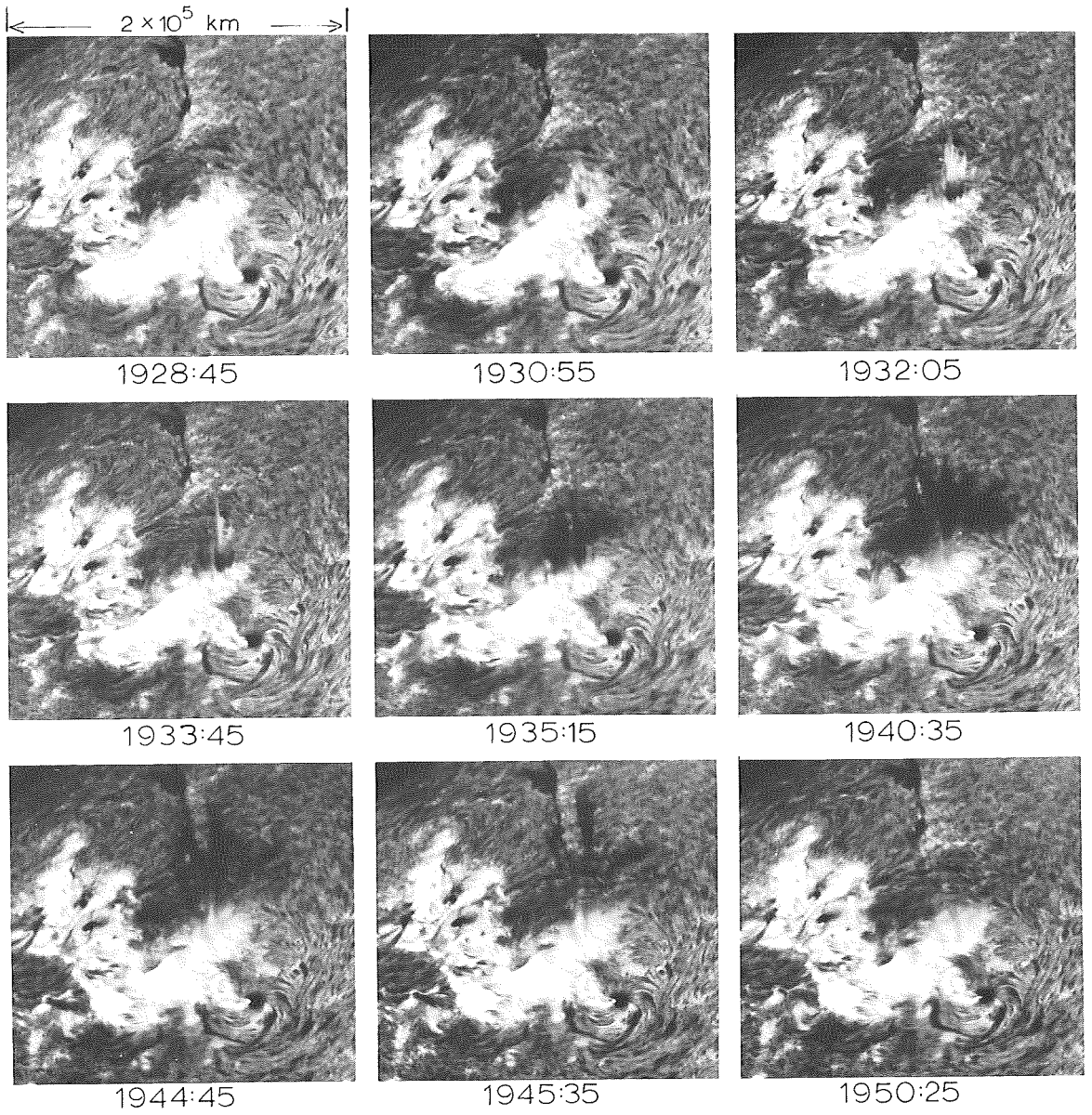


Figure 15. A fan-shaped surge occurring with a flare on 21 May 1967. It is seen that the development of the surge is coincident with a late increase in the radio event in Figure 14.

## 4.2 Type II Bursts and Flare-waves

For over half a decade, it has been conjectured that flare waves are generated by the same cloud of ions which produce Type II bursts (Wild 1963; Kundu, 1954; Lin and Anderson 1967). Also, much theorizing has been done on the nature of waves (Anderson 1965, Meyer 1968, Uchida 1968), but very little observational material has been offered to substantiate or negate these conjectures.

The list of flare waves discussed in Section 2.3 were checked for the occurrence of Type II events during these flares from reports in Solar-Geophysical Data. Eighteen of the 50 (36%) events for which spectral radio observations were available, were found also to have associated Type II bursts. It is interesting to note that prior to 1963, 7 of 29 wave events (< 25%) were associated with Type II bursts while since 1963, 11 of 21 wave events (> 50%) were associated with Type II bursts. This increase in the percent of concurrent waves and Type II bursts is attributed to improved radio spectrum observations.

To determine whether or not Type II events were really absent when no Type II is reported, it is necessary to carefully scrutinize the actual radio spectra. Fourteen radio spectra were available from the Harvard Radio Astronomy Observatory at Fort Davis, Texas during flares which also produced waves. 9 of these radio spectra showed strong Type II events; 2 were such weak Type II's as to be almost invisible; 3, at best, could be considered questionable Type II events. It seems probable that weak Type II events might easily be obscured on days having long duration noise storms (Type I) or when a Type II event occurs in rapid succession after an earlier major flare. However, for the 3 questionable Type II events neither of these conditions existed.

Further evidence for associating waves and Type II events can be sought by comparing the timing and velocities of individual events. The clearest example of a wave that has been observed at Lockheed occurred on 20 Sep 1963.

Photographically subtracted observations at H-alpha $\pm$ 0.5Å of the event are shown in Figure 16 below the corresponding radio spectrum. It is obvious that the timing of the wave with the Type II is very precise. The start of the explosive phase of the flare occurred at 2056:15 U.T. $\pm$ 15 sec. At exactly this same time a very broad Type III occurs throughout the radio spectrum, similar to an event described by Dodson and Hedeman (1968). As shown in Section 2.3, the beginning of the explosive phase is also the time at which the wave events are typically initiated during flares. The occurrence of a Type III marking the start of the explosive phase was an occasional but not a frequent characteristic in the radio records surveyed. The Type II event began at approximately 2059:15 U.T. at 200 Mc/sec, 3 minutes after the start of the explosive phase.

It is not clearly established from this limited study that the generation of waves and Type II events are necessarily related. Additional Type II records should be studied for the correspondence in time and velocity between individual wave events and Type II bursts. Also such a study should not neglect the existence of sprays of material from a flare. Sprays may have velocities comparable to waves and Type II events and they may be observed at the same time during flares. Consequently, observed or inferred heights for sprays, waves, and Type II events could be compared.

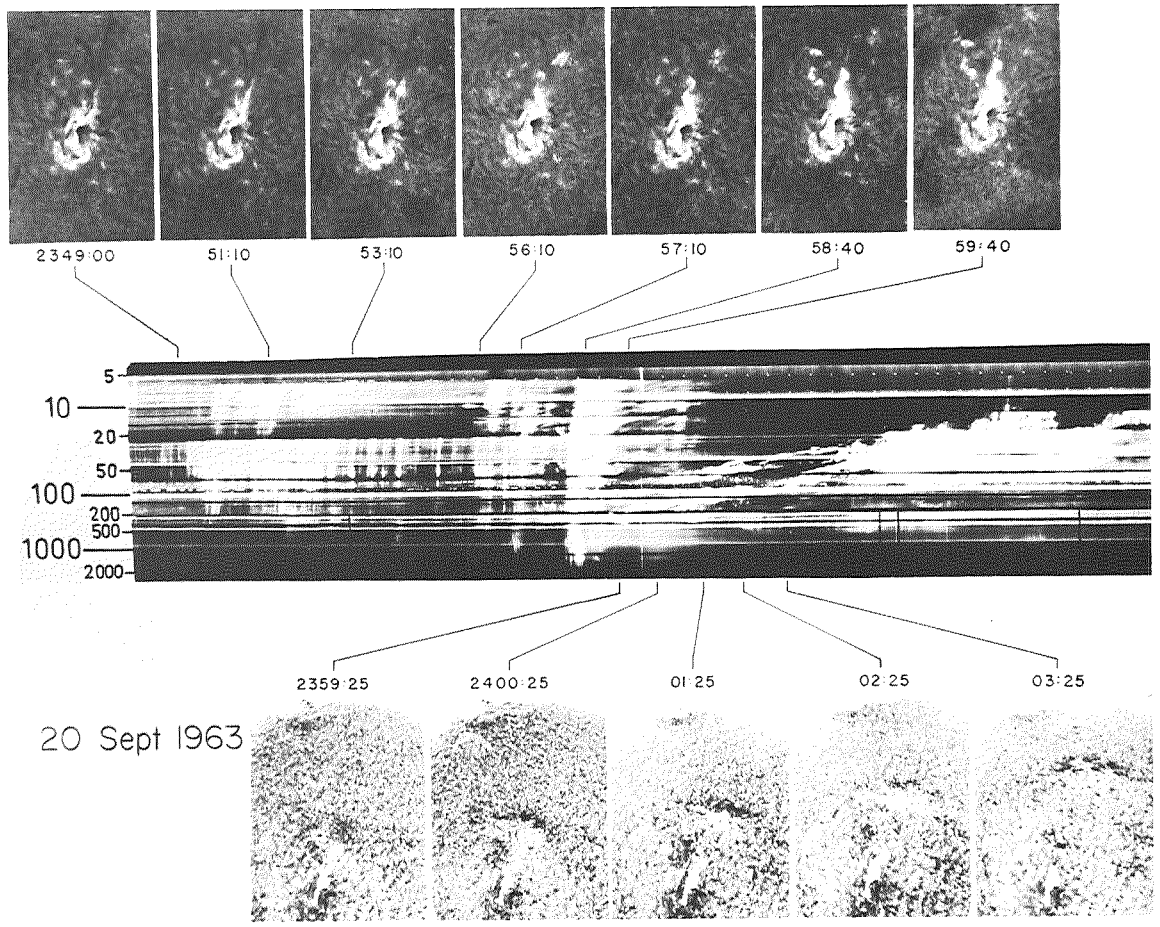


Figure 16. A comparison of the wave event and Type II burst associated with the flare on 20 September 1963.

# Section 5
# SOME PARTICLE EVENTS AND H-ALPHA FLARE CHARACTERISTS

## 5.1 Flare Waves and Prompt Solar Electrons

For the years 1964 and 1967, 120 prompt electron events with a maximum flux $\gtrsim$ 40 keV have been tabulated by Lin (Lin and Anderson 1967, 1968). During the same period, 16 flares observed at the Lockheed Solar Observatory produced visible effects on chromospheric features due to a high speed disturbance, presumably due to a shock wave. Only 8 of the 16 flares having visible wave effects were also associated with the arrival of prompt electrons near the earth. Since prompt electrons strongly tend to be associated with flares on the western hemisphere or center of the solar disk, (Anderson and Lin, 1967) one might anticipate that the flare-wave events not associated with observed prompt electrons might tend to occur on the sun's eastern hemisphere. This is not the case, however, as is shown by the distribution of wave events in Figure 17. There are 6 flare-wave events without observed prompt electrons to the west of central meridian and only 3 to the east of central meridian.

The wave events which are associated with the same flares as prompt electron events are distributed near the center of the disk. The wave events tend to have the same distribution of the solar disk as Type C (complex) rather than Type S (simple) prompt electrons (Lin and Anderson, 1967). These 8 events nearly all occur too far east to be associated with Type S prompt electrons. In fact 6 of the wave-events were associated with Type C prompt electrons and 2 with questionable Type S electrons. All eight events occur between $15^{\circ}$ W and $35^{\circ}$ E of central meridian while only one wave-event not associated with prompt electrons falls in this range. Since this event occurs immediately after 2 other flares also with prompt electrons, it may have been obscured by the high electron fluxes from the earlier events.

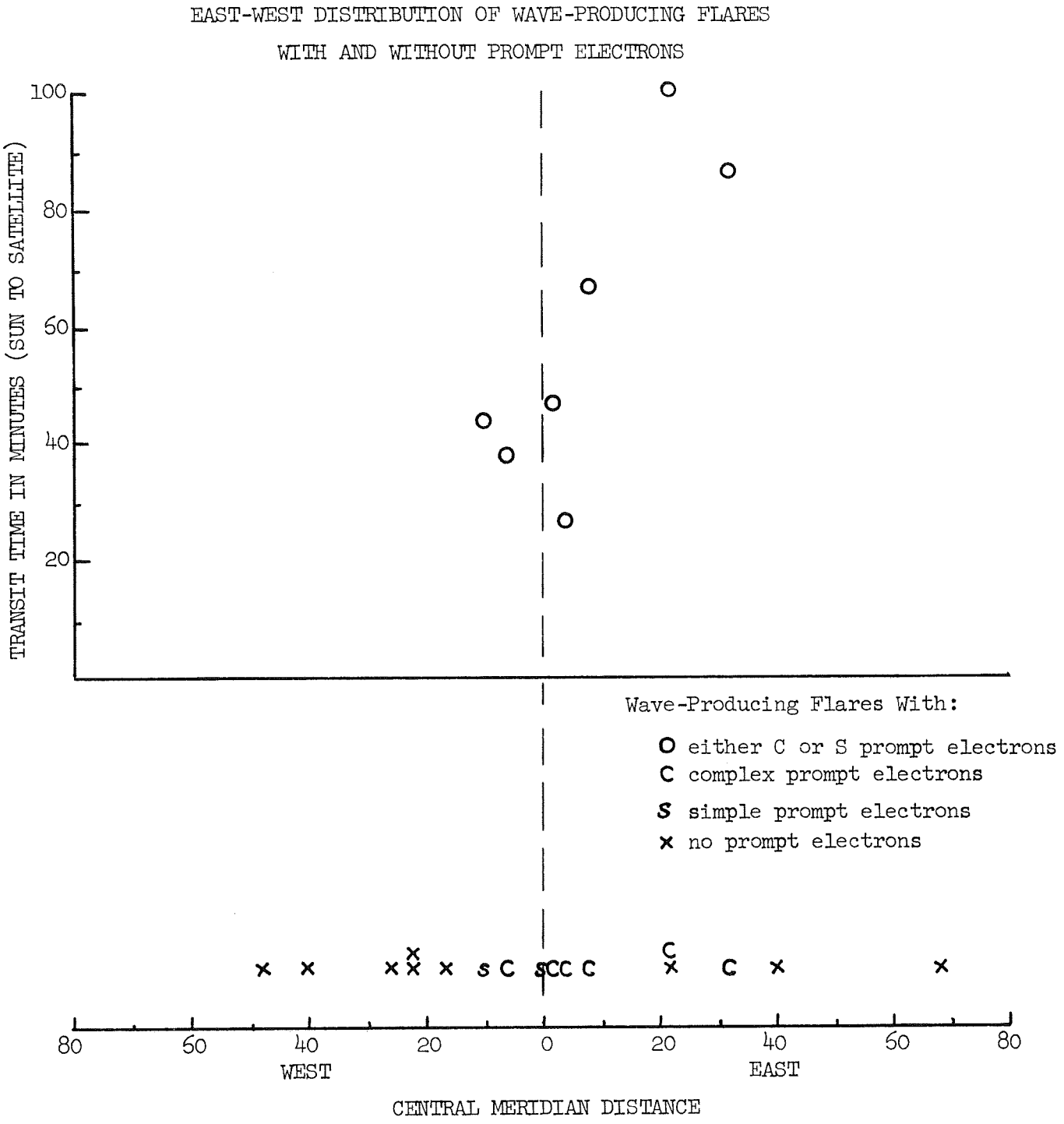


Figure 17. Distribution of flares which produced wave-effects and for which data on prompt electron events was available. Prompt electrons are shown as either Complex (C) or Simple (S).

From these data, there is no identity one can establish between flares producing visible wave effects and those for which Type S prompt electrons are observed. An identity between waves and Type C prompt electrons is possible but no physical relationship is suggested. It may only be that both events are detectable from very energetic flares.

Possible relationships between delayed electron and proton events and waves should be studied. Wave velocities average from 710 to 880 Km/sec (Section 2.3) and therefore they are more likely to be associated with much slower particles than the prompt electrons or protons. Also the range of wave velocities varies mostly within a factor of 2 and is thus similar to the dispersion in transit times for the delayed electron and proton events.

## 5-2 Particle Injection Into Interplanetary Space From Solar Flares

This section is devoted purely to conjecture. Little is known of the mechanisms by which protons and electrons are released during solar flares and perhaps little can be learned directly from optical observations of flares. However, the Lockheed high resolution observations of active regions do present some flare details worthy of discussion relating to possibilities for the time and duration of the injection of particles observed in space.

Lin and Anderson (1967) show that there are 2 distinct classes of particle events detected from the same flares; prompt events, generally observed within an hour of the start of a flare, and delayed events observed on the order of 30 hours after flare start. H-alpha observations show two distinctly different aspects of flares which could be associated with separate mechanisms releasing prompt and delayed particles. These are the phase of developing flare points and the flash phase or explosive phase of the flare.

In Section 2.2 it was shown that the start of a flare and the explosive or

flash phase often are not coincident in time although the explosive phase usually occurs within 10 minutes after flare start. It is shown also in Section 2.3 that the initiation of the wave phenomenon is identified with the start of the explosive phase rather than flare start.

The long standing speculated association of Type II radio bursts with waves was further amplified in Section 4.2. The velocities of waves and Type II bursts is appropriate for relating their generation to the same outburst of particles seen later as delayed events. In addition to waves, most rapid ejections observed with solar flares, such as sprays and some filament eruptions, have observed velocities well below 2000 Km/sec. Therefore, these ejections are most likely to be associated with the arrival of delayed particle events reaching the earth approximately 20 or more hours after the solar event.

None of the rapid ejections attain excape velocity prior to the explosive phase of the flare. The start of the explosive phase, therefore, is the earliest time at which any of the observed ejections are able to escape the gravitational field of the sun although the outward ascent of material may be observed even before the start of the flare as in the case of erupting filaments, (Smith and Ramsey, 1964). These rapid visible ejections are generally no longer visible in the immediate vicinity of the flare by the time it has attained maximum intensity. Flare associated events observed after flare maximum do not have sufficiently high velocities to be considered in this discussion. Consequently, the time between the start of the explosive phase and the maximum of the flare is probably the maximum length of time during which the delayed particles are able to escape the region of the flare.

There are no visible ejections from solar flares with sufficient velocities to suggest a possible relationship to the ejection of prompt electrons. The relativistic velocities of Type III bursts, however, suggests that Type III's could be generated by prompt electrons leaving the vicinity of a solar flare.

Of all the observed phenomena associated with flares at optical wavelengths, there is only one characteristic which might possible be related to Type III bursts and consequently to the ejection of prompt electrons. That characteristic is the development of flare points. The development of flare points begins at the start of the flare and may continue throughout most of the life of a flare. This process is not necessarily related to the explosive phase or flash phase of a flare except that more flare points may develop at that time. Similarly, Type III bursts are seen at the onset of many flares but may be sporadically observed through the maximum of a flare, sometimes superposed on Type II bursts (Wild 1963). Ocassionally, a strong group of Type III's will coincide with the onset of the flash phase (Dodson and Hedeman, 1968) as also shown in Figure 17, Section 4.2. Like flare points, however, the occurrence of Type III's is not unique to explosive phase of flares. Thus, the timing and sporadic occurrence of Type III bursts tempts one to associate them with the development of flare points while the velocities of Type III bursts suggests an association with the ejection of prompt electrons. If this conjecture is plausible, then one would also infer an association between the development of flare points and the ejection of prompt electrons. It could follow, then, that the ejection of prompt electrons would begin at the onset of a flare and continue as long as new flare points are developing. If we regard a flare as an envelope of short-lived developing and decaying flare points with lifetimes of 3 minutes or less as discussed in Section 2.1, and suppose that flare points are related to the same phenomenon which generates prompt electrons, then it could also follow that the ejection of prompt electrons may continue for most of the duration of the flare in H-alpha. This hypothetical argument might be confirmed or negated by studying numerous flare points observed 2 to 4 Angstroms into the red wing of the H-alpha line, preferably in real time on a television monitor. Such observations could then be related to the occurrence of Type III bursts.

In summary it is suggested that:

1) Waves and rapid visible ejections from solar flares may be associated with delayed particle events and Type II bursts.

2) The development of flare points may be associated with prompt particle events and Type III bursts.

## ACKNOWLEDGEMENTS

We thank Mr. Arthur Covington for making the 2800 MHz radio data available, Mr. Paul Gagnon for verifying some of the very small 2800 MHz events, Mr. Donald Horan for assistance in interpreting the OGO IV x-ray data, Dr. Robert Lin for his list of recent prompt electron events, and Dr. Alan Maxwell for the Harvard solar radio spectra. We especially want to thank the persons named in the text for supplying the data described herein.

## Section 6
## REFERENCES

Anderson, G., Dissertation, University of Colorado, Boulder, Colorado (1966)

Angle, K. L., Astron. J. 73

Arnoldy, R. L., S. R. Kane and J. R. Winckler, Sol. Phys. 2, 171-8 (1967)

Arnoldy, R. L., S. R. Kane, and J. T. Winckler, Ap. J. 151, 711 (1968)

Castelli, J. P. and G. A. Michael, Sol. Phys. 1, 127 (1967)

Dodson, Helen W. and E. Ruth Hedeman, Sol. Phys. 4, 229-239 (1968)

Donnelly, R. G., ESSA Tech. Report ERL 86-SDL3 (1968)

Donnelly, R. F., J.G.R. 74, 1873-7 (1969)

Drake, J. F., Sr. J. Gibson, and J. A. Van Allen, Iowa Catalogue of Solar X-Ray Intensity (July 1968)

Ellison, M. A., Mon. Notices of R.A.S. 109, 3 (1949)

Erickson, W. (private communication)

Hyder, C. L., Sol. Phys. 2, 267-284 (1967)

Lin, R. P. and K. A. Anderson, Sol. Phys. 1, 446-464 (1967)

Lin, R. P. and K. A. Anderson (List of Events, private communication, 1968)

Kundu, M., Solar Radio Astronomy, Interscience, John Wiley and Sons, New York (1965)

Meyer, F., I.A.U. Symp. on Structure and Development of Solar Active Regions, ed. Kiepenheuer, 485-489 (1968)

Moreton, G. E., AAS-NASA Symp. on the Physics of Solar Flares, NASA-SP-50, 209-212 (1963)

Ramsey, H. E., S. F. Smith and K. L. Angle, Final Report, High Resolution Photography of Solar Flares, Lockheed Missiles and Space Company Report, 681495 (1968)

Richmand, A. (private communication)

Smith, S. F., and H. E. Ramsey, Z. Astrophys. 60, 1-18 (1964)

REFERENCES (Cont.)

Van Allen, J. A., J.G.R. 72, 5903 (1967)

Van Allen, J. A., Ap. J. 152, L85 (1968)

Wild, J. P., AAS-NASA Symp. on the Physics of Solar Flares, NASA-SP50, 161-177 (1963)

Uchida, Y. (personal communication, 1968)